Title
Surface modification of enamel using near-UV laser irradiation

Author
Wheeler, Cameron R.

Publication Date
2002

Peer reviewed|Thesis/dissertation

Surface Modification of Enamel Using Near-UV Laser Irradiation

by

Cameron R. Wheeler

THESIS

Submitted in partial satisfaction of the requirements for the degree of

MASTER OF SCIENCE

in

Oral Biology

in the

GRADUATE DIVISION

of the

UNIVERSITY OF CALIFORNIA

San Francisco

[redacted]

Date

University Librarian

I. ACKNOWLEDGEMENTS

I would like to thank the following individuals who contributed so much in helping me complete this project:

Dr. Daniel Fried, my mentor for his thoughtful guidance and direction throughout all aspects of this project. I am grateful for his patience and friendship.

Dr. John Featherstone and Dr. Sally Marshall for their time and consideration in reviewing my progress with the project. Their expertise and constructive criticisms were most appreciated.

John Xie and Charles Le, my research colleagues, for providing technical lab assistance (*par excellence*) without which this project would not have been completed.

Larry Watanabe for his abundant support with the imaging aspects of this project, and other endeavors throughout my dental school education.

Dr. Art Miller for his enthusiastic contributions to the design of this project

Most importantly, I would like to thank my wife Tatiana and my son Dimitri for their unconditional love and support. Their sacrifices throughout my educational pursuits at UCSF are not forgotten. They have been the driving force in my life, always keeping me on an even keel.

II. ABSTRACT

Surface Modification of Enamel Using Near-UV Laser Irradiation

Cameron R. Wheeler, D.D.S.

Lasers can be used to modify the surface of dental enamel to increase the bond strength to restorative materials and to render the mineral phase more resistant to acid dissolution. Previous studies have suggested a synergistic relationship between CO_2 laser irradiation and fluoride treatment on increased resistance to acid dissolution. In this study a near-ultraviolet (UV) laser operating with λ=355 nm laser pulses of 5 nanosecond duration was used to modify the surface morphology of dental enamel to increase the bond strength to restorative materials and increase the uptake of topical fluoride to render the surface more resistant to acid dissolution. The hypothesis that was tested is that short UV laser pulses are primarily absorbed by protein and lipid localized between the enamel prisms resulting in removal of intact mineral producing etching of the surface without thermal modification of the mineral phase. Such modification is likely to increase the permeability of the enamel surface and the subsequent absorption of fluoride. In addition, there is an increase in surface roughness without the formation of a layer of loosely adherent, thermally modified enamel that increases the bond strength to composite restorative materials. The surfaces of blocks of bovine enamel, 5 x 5 mm^2, were uniformly irradiated by 355-nm laser pulses and subsequently bonded to composite. The shear bond test was used to assess the bond strength of non-irradiated blocks (negative

control), acid-etched blocks (positive controls), and laser-irradiated blocks. The laser treatment significantly increased the shear-bond strength of composite to enamel, to a level two-thirds of the conventional acid etch, comparable to bond strengths achieved with glass ionomer cements. Bovine enamel surfaces irradiated by the same laser were evaluated for resistance to acid dissolution. Groups included no treatment, fluoride only, laser treatment only, and fluoride and laser treatment. Neither the laser alone, nor the fluoride alone significantly increased the resistance of the initially sound enamel to acid dissolution. The laser treatment, followed by a topical application of fluoride, increased the resistance to acid dissolution by approximately 55% over controls. In conclusion, a novel method was demonstrated for increasing bond strength to restorative materials and enhancing fluoride delivery to enamel surfaces and shed some light on the underlying mechanisms on caries inhibition via laser treatment and topical application of fluoride.

TABLE OF CONTENTS

LIST OF FIGURES

LIST OF TABLES

III. INTRODUCTION

A. Background

a. History of the laser in dentistry

Since Theodore H. Maiman (Hughes Research Laboratories; Malibu, CA) developed of the first working laser, the ruby laser with a wavelength of 0.694-μm in 1960, there has been great interest among dental practitioners, scientists, and patients to make lasers a viable clinical adjunct in the everyday dental practice. The focus of this interest is that the laser can assist the dentist in multiple ways and tasks to deliver dental treatment in an efficient and pleasant manner.

Many researchers have explored the use of lasers to intentionally modify the surfaces of teeth to improve bonding of dental restorations. [1-4] Until recently, dental lasers were viewed skeptically by many practitioners, and considered useful in only limited soft-tissue procedures. However, new lasers that are more efficiently absorbed by dental hard tissues have become available. Presently, lasers of varying kinds have been indicated for use in the clinical setting including soft tissue ablation, curing of dental restorative materials, activating bleaching compounds, cleaning and sterilizing root surfaces and root canals, promoting caries resistance, identifying carious lesions, removing carious tissue, and preparing conservative cavity preparations.

To date, the Food and Drug Administration (FDA) has approved five laser systems for clinical use in dentistry. They are the CO_2, the Argon, the Erbium: Yttrium-Aluminum-Garnet (Er:YAG), the Holmium: Yttrium-Aluminum-Garnet (Ho:YAG), and the Neodymium: Yttrium-Aluminum-Garnet (Nd:YAG) lasers. Several manufacturers have received clearance for argon lasers to activate tooth-bleaching solutions and cure composite resins, while the CO_2 laser has been widely used in operative situations involving soft tissues to cauterize blood vessels, perform biopsies, remove benign and malignant tumors, treat gum disease, and perform gingivectomies.

Several lasers have received clearance for hard tissue application use on teeth. On May 7, 1997, the Food and Drug Administration cleared the first laser system for treating tooth decay, the Centauri Hard-tissue laser (an Erbium:YAG laser), made by Premier Laser Systems (Irvine, CA). Recently, American Dental Technologies (Corpus Christi, TX) received FDA clearance to market its PulseMaster 600 IQ laser (a free-running, pulsed Nd:YAG at λ =1064 nm) for first degree caries removal; to date it has not yet been cleared to remove intact enamel or dentin tooth structure. BioLase Technology's (San Clemente, CA) Millenium HydroKinetic Erbium laser has received FDA clearance for all class of cavity preparations, and for all age groups. The continuum Er:YAG laser was the first laser approved for use on children.

Expansion in the use of lasers for specific tasks in the dental practice has occurred and will continue to occur over the next few years requiring the identification of optimal operating parameters of these lasers (wavelength, pulse

rate, spot size, and beam intensity, etc.) to maximize efficient delivery of laser energy and to reduce any harmful side effects, including enamel fracturing, charring, and excessive heat accumulation in the pulp. Further evolution in the size and portability of the laser delivery system, including the development of a user-friendly, lightweight, and compact delivery handpiece, will greatly facilitate the ease and acceptance of the laser in clinical dentistry.

b. Laser physics and hard tissue optics

There are many factors that determine the interaction between laser and tissue. This includes the optical properties of the tissue such as transmission, absorption, scattering, and reflection of light. The optical properties are expressed by the refractive indices of the tissue (n_r, k), the scattering and absorption coefficients (μ_s and μ_a), the reflectance (R), and the scattering anisotropy. [5-7]

The irradiation parameters of the laser, such as wavelength, repetition rate, pulse duration, pulse energy, beam size, delivery method, and temporal characteristics of the laser beam also effect the laser-tissue interaction. The two most important factors are wavelength and pulse duration. In the determination of how light affects tissue, wavelength determines the "quality" or type of interaction between the laser and the tissue. The amount of energy, or the *intensity* of the beam, and tissue properties determine the "quantity" or extent of the interaction. The ultimate effects of laser irradiation on tissue depend on the

distribution of the energy inside the tissue. The temperature rise within the irradiated tissue is a balance between energy deposited in a specific time, and energy conducted away as heat. The temperature rise determines the extent of chemical and morphological changes of the tissue. [7-9]

Absorption and scattering coefficients are determined experimentally, and are given values of reciprocal centimeters (cm^{-1}). These coefficients for enamel have been well documented in the literature. [10] In tissues with a high absorption for a specific wavelength, little or no scattering occurs, and the overall energy of the incident beam is deposited within the first few micrometers of the tissue surface. This energy is converted to heat that is conducted away from a superficial surface zone. The laser parameters of pulsed versus continuous emission, pulse duration, pulse repetition rate, as well as the thermal conductivity and heat capacity of the tissue itself, determine if the heat generated by the laser interaction with the tissue is contained or diffused.

Scattering (deflection of light in different directions inside the tissue mass so that it is lost from the original beam) usually produces no biologic effect, but can transfer heat to adjacent tissues including the dental pulp, and cause unwanted thermal damage, resulting in subsequent pulpal death. It should be noted that dentin and enamel have different optical properties; so for a given wavelength, it may have negligible absorption in the enamel, but high absorption in the dentin, causing deleterious effects.

The spectral output of the CO_2, the Er:YAG, and the Er:YSGG (Erbium: Yttrium Scandium Gallium Garnet) laser systems exhibit high absorption in

enamel. The CO_2 laser (operating at wavelength 9.3-, 9.6-, 10.3-, or 10.6-μm) shows strong absorption with the inorganic mineral component of enamel. The spectral output of the Er:YAG (λ=2.94-μm) laser overlaps that of free water, and the Er:YSGG's (λ=2.78-μm) spectral output overlies hydroxyl (OH^-) group within the hydroxyapatite (HA) crystals. The Nd:YAG (frequency tripled—third harmonic--at λ=355 nm) and some of the excimer, or "*excited-dimer*", lasers (containing a diatomic molecule usually of an inert gas atom and a halide atom) including the Argon Fluoride, ArF, (λ=193 nm), the Krypton Fluoride, KrF. (λ=248 nm), and the Xenon Chloride, XeCl, (λ=308nm) lasers, show spectra that overly that of the peptide bond (OC-NH) of protein. [11] The Nd:YAG laser, operating at 1064 nm, shows no or minimal overlap with the enamel spectrum, and therefore is not suitable for enamel tissue modification unless extremely high fluences are used. Early laser systems using this wavelength were clinical failures with hard tissue application. [12]

c. Bonding of orthodontics brackets and attachments and dental restoratives

M. G. Buonocore's acid-etch technique utilizing ortho-phosphoric acid, introduced in 1955, provides mechanical bonding between the composite restorative material and the treated enamel surface. [13] Today this technique is recognized as a fundamental step in the placement of dental composite restorations to enamel surfaces. Further advancements in dental restoratives

depend on improving the bond between the tooth surface, the dental adhesive, and the resin composite. This bond must be durable, biocompatible, and impervious to oral fluids.

Buonocore's acid etching of enamel is a tried and well-understood technique. Enamel is a very highly mineralized material containing approximately 3% water and 1% organic (protein and lipid) material by weight. The mineral, predominantly carbonated apatite, exists as crystals that are packed together to form interlocking "rods" or "prisms" of approximately 4-5 microns in diameter. When an acid is applied to the enamel surface over a short duration of 15-30 seconds, the acid dissolves the highly mineralized prisms more than the inter-prismatic boundaries located between the prisms, resulting predominantly in what has been termed a type 1 etch pattern. [14] (A type 2 etch pattern can be sometimes simultaneously seen with type 1 pattern, depending upon surface morphology. Thus, the roughness of the surface is increased at a microscopic level, with troughs formed between 10 and 30 micrometers deep. A longer etch time actually results in a different etch pattern, unfavorable because it is deeper but not necessarily more rough. [14, 15] When an unfilled, low viscosity resin is placed on this surface it penetrates into these troughs or pores forming "resin tags". When the resin cures, these tags become solid and so are locked in place. As a result, a strong micro-mechanical bond is formed between the resin and the enamel.

A widely accepted clinical procedure is to use an etchant containing ortho-phosphoric acid at a concentration of about 35 to 40%. The application time of acid to achieve a clinically successful bond is of the order of seconds, usually between 15 and 30 seconds. A longer etch time does not result in a deeper, stronger etch pattern; rather it simply removes more enamel structure. [16, 17] Highly fluoridated enamel, which by nature is more resistant to acid-challenge, and primary deciduous teeth, which have a different enamel structure, needs consequently, longer etch times. [18]

The enamel surface, when well dried, reveals a frosted white, etched appearance before resin is applied, suggesting an increased degree of surface roughness and subsequent change in optical properties. When the composite restorative material is placed and then polymerized in contact with the resin/enamel layer, a chemical reaction takes place between the composite and the resin. Thus, the composite has been 'bonded" to the enamel surface.

In the early 1970's, the orthodontic community capitalized on this new bonding technology. Direct bonding of orthodontic brackets and attachments, following this etching procedure, replaced the days of laboriously banding each individual tooth. This application of bonding technology, with the advent of pre-adjusted, "straight-wire" appliances, single-handedly moved the field of orthodontics into the modern era.

d. Demineralization of enamel around orthodontic appliances

An unfortunate side effect of bonded orthodontic attachments is the development of white spot lesions on the surfaces of teeth, often noted at the time of appliance removal. [19] The formation of a white spot lesion is the first discernable clinical sign of dental caries. A white spot lesion is formed in response to loss of mineral from the enamel due to long-standing acid production from oral microbes contained in dental plaque that typically accumulates along the periphery of orthodontic attachments. [19, 20]

Loss of mineral changes the optical characteristics of the normally translucent enamel to an opaque tissue, due to the disruption in the transmission of light through the mineral matrix. White spot lesions are unaesthetic and difficult to reverse even when the best hygiene and management strategies are employed. Zachrisson reported that the incidence of white spot lesions among orthodontic patients exceeded 15% of the cases studied. [22] While white spot lesions may form anywhere in the mouth, they are most commonly seen around the periphery of brackets, around the gingival margins of the teeth, under bands where bonding material has been eroded, and where excess resin cement has been incompletely removed. The highest prevalence was noted on the first molars, the mandibular canines, mandibular premolars, and the maxillary lateral incisors. [23, 24] Only with diligent removal of plaque through proper oral hygiene technique can one remove these cariogenic oral microbes from the non-self cleaning, difficult to reach areas around orthodontic appliances.

e. The role of fluoride

The ability of fluoride to prevent and arrest the caries process has been well established. [25] Vast reductions over the past 25 years in the numbers of decayed, missing, and filled teeth have been directly associated with the fluoridation of public waters, and widespread use of fluoride containing dental products (dentifrices, mouthwashes, rinses, and topical gels). [25, 26]

Fluoride has been identified to be beneficial in arresting and reversing the caries process by three separate mechanisms. [27] First, when the dental plaque is acidified due to bacterial production of acids, a portion of the fluoride present in the plaque fluid combines with the hydrogen ions to form hydrogen fluoride (HF). The ionized form of fluoride (F^-) is unable to cross cell walls of cariogenic bacteria, but the HF form is able to freely pass through the cell walls. Once inside the cariogenic bacteria, the HF dissociates, thus acidifying the intracellular environment and releasing the fluoride ion (F^-), that interferes with important enzymatic activities of the bacterium. [27] Specifically, fluoride ion has been implicated in disrupting enolase, an enzyme essential for the metabolism of carbohydrates. [28]

Second, fluoride is active in the inhibition of the demineralization process. Fluoride present in the aqueous solution surrounding the apatite crystals of the tooth mineral is adsorbed strongly to their surface, and protects it from acid dissolution taking place in the subsurface of the tooth. [29] Only fluoride that

originates from plaque fluid via topical sources exhibits a measurable inhibitory effect on demineralization. Fluoride incorporated in the tooth mineral at the time of tooth development is insufficient to produce any caries protection. This necessitates a lifetime of regular topical fluoride application to ensure caries protection. [28]

Third, fluoride enhances the mineralization process by initiating a cascade of events. It is initiated by the fluoride ion adsorbing to the crystal surface. The negative charge associated with the fluoride ion is strongly attracted to the positive atoms (Ca^{2+}) within the enamel crystal structure. Its negative charge further attracts additional calcium ions (Ca^{2+}), which in turn attracts negatively charged phosphate ions (PO_4^-), leading to the growth of new apatite crystals. [28]

Saliva is super-saturated with calcium and phosphate ions, as well as containing acid-neutralizing components and anti-bacterial elements necessary for maintaining the integrity of the dental tissue. [30] The partially demineralized crystal surfaces within the subsurface lesion act as nucleators and give rise to new surfaces on the crystals. [28] With the presence of fluoride in the saliva, these new crystals are predominantly made of fluorapatite (FAP), which has a much reduced solubility level in acid, as compared to original carbonated apatite mineral, carbonated hydroxyapatite mineral, and pure hydroxyapatite (HAP) mineral ($Ca_{10}[PO_4]_6[OH]_2$).

f. Previous laser-bonding and surface modification studies

The use of the CO_2 laser has been widely studied on its effect on enamel mineral composition of dental hard tissue.[6-9, 20, 27] Kantorowitz used the CO_2 laser, at four wavelengths between 9.3- and 10.6-μm and fluences between 3.5 J/cm^2 and 9.5 J/cm^2, to study the ability of laser irradiation to roughen the surface of enamel to enhance the bonding of composite resin (Transbond XT Light Cure Adhesive Paste; 3M Unitek, Monrovia, CA) resin and glass-ionomer (Fuji Ortho LC; GC America; Alsip, IL) bonding agents. Shear bond testing, utilizing orthodontic attachments and commercially available orthodontic bonding agents, was the method used to quantify the degree of bonding. In addition, scanning electron microscopy served as an adjunctive tool in quantifying and qualifying the microscopic nature of the bond. He noted that while no treatment group matched the bond strengths of acid etched controls (20.8 MPa for resin composite; 13.2 MPa for glass ionomer) the effect of laser irradiation improved the strength of the bond above that of the non-treated controls (1.1 MPa). [31] An increase in fluence appeared to provide a slightly beneficial increase in bond strengths. The mean bond strengths for the low fluence groups (3.5 J/cm^2 and 5 J/cm^2) averaged approximately 3.1 MPa for the composite and 7.7 MPa for the glass ionomer. By using higher fluences (9.5 J/cm^2) bond strengths were increased to 11.8 for the composite and 8.4 for the glass ionomer. [31] He noted, however, that there were fluence-dependent alterations in the surface structure of the irradiated enamel surfaces, notably in the degree of enamel crystal melting and fusion, and in the appearance of exfoliation and pitting. [31]

The well-designed research protocol in Kantorowtiz's research served as a model for the present study. The aforementioned results would serve as a valuable reference for the findings of the present study, where instead of the CO_2 laser, the treatment would be provided by a frequency-tripled Nd:YAG laser system operating at 355 nm.

Ariyaratnam *et al.* used a pulsed Nd:YAG laser system operating at 1064-nm and found disappointing shear bond test results, ranging from 4.6 to 8.8 MPa. [32] Since there is little surface absorption in enamel of the Nd:YAG laser (λ=1064 nm), little surface modification would be expected, insufficient to guarantee an clinically successful bond.

Fuhrmann *et al.* studied the effects of the CO_2 and Nd:YAG lasers on enamel conditioning and orthodontic bracket bonding by measuring *in vitro* tensile bond strengths (using vertically applied forces). [33] The highest laser-treated *tensile* bond strengths were seen with the Nd:YAG laser treated samples (4.1 MPa). Comparable values were seen with the CO_2 laser-treated group (3.3 MPa) and with the acid-etch treated control (4.9 MPa). They concluded that the CO_2 and Nd:YAG dental lasers used produced satisfactory enamel conditioning to achieve tensile bond strength sufficient to meet the requirements of bracket bonding. [33]

Martinez-Insua *et al.* studied the tensile strength of bracket-tooth bonds obtained after preparation of the surface for adhesion by conventional acid-etching and by Er:YAG laser etching (four 200 mJ pulses per second). Mean tensile bond strength for acid-etched enamel (14.05 MPa) was significantly

higher than for laser-etched enamel 8.45 MPa). SEM studies of both resin-enamel interfaces suggested bond failure after laser etching was due to micro-cohesive fracture of tooth tissue, coupled with unfavorable and extensive subsurface fissuring secondary to excessive incident energy. [34]

Stratmann *et al.* used 193 nm ArF-excimer laser irradiation (energy density of 260 mJ/cm^2) to selectively [11] modify the surface of enamel in preparation for orthodontic bonding. The observed tensile bond strengths were 6.6 MPa in the laser-treated group and 8.8 MPa in the acid-etched group. [35]

Hsu *et al.* studied the effects of enamel demineralization by combining high-energy, continuous-wave CO_2 (λ =10.6-μm) laser irradiation with partially saturated, fluoride containing (0.2 ppm fluoride) demineralizing solution. [36] Dissolution of enamel, in the presence of a buffered lactic acid solution (pH 4.5), can be significantly reduced when the enamel has been irradiated with a continuous-wave CO_2 laser (10.6-μm). [37] Hsu *et al.* demonstrated that combining the beneficial effects of fluoride with laser-irradiated and modified enamel synergistically enhanced the level of acid resistance. [36] Dental enamel mineral, which is comprised of carbonated apatite, is amenable to surface conversion to fluorapatite after laser irradiation, in the presence of fluoride ion. [38] Tagomori *et al.* reported that APF application *after* Nd:YAG laser irradiation produces a greater fluoride uptake in enamel than APF application *before* laser treatment.[39]

B. Overall Hypothesis and Purpose

The purpose of the project is to study and evaluate the effects of laser irradiation at wavelengths resonant with protein and lipid absorption bands on the microscopic morphology of enamel, by selectively targeting and ablating these organics from the intact apatite crystal matrix, and to evaluate changes in 1) *in vitro* shear bond strengths of resin bonded orthodontic attachments, and 2) *in vitro* caries resistance to acid challenge.

The central hypothesis of this research is that frequency-tripled Nd:YAG lasers (λ = 355 nm), operating at wavelengths resonant with specific absorption bands, can selectively modify susceptible tissue components in the heterogeneous structure of enamel, resulting in apparent surface morphological changes (without alteration of the chemical structure of the enamel mineral) to achieve: 1) clinically acceptable *in vitro* shear bond strengths of orthodontic attachments; and 2) augment fluoride delivery to improve *in vitro* dissolution resistance from acid challenge.

C. Specific Aims

a. Specific Aim #1: Test the hypothesis that a frequency-tripled Nd:YAG laser (λ = 355 nm) can modify the surface structure of enamel to improve bonding strengths of dental composite resins when compared to both unmodified/unetched samples and traditional acid etched and bonded samples.

b. **Specific Aim #2:** Test the hypothesis that a frequency-tripled Nd:YAG laser (λ = 355 nm) can selectively remove protein from the crystalline structure of enamel tissue, resulting in a surface modification that will enhance fluoride delivery to augment resistance to acid challenge.

c. **Specific Aim #3:** Test the hypothesis that frequency-tripled Nd:YAG laser (λ = 355 nm) ablation does not adversely alter the chemical structure of the hydroxyl- and carbonated-apatite mineral, while changing the microscopic enamel surface morphology.

IV. MATERIALS AND METHODS

A. Specific Aim #1: Shear Bond Strength Testing

a. Rationale

Although pure shear force does not occur clinically in the oral cavity, nor alone is it the cause for clinical failure of an orthodontic attachment, the shear bond strength is used as an indication of the suitability of the bond to withstand the intra-oral forces during orthodontic treatment. The methods used for measuring bond strengths are not standardized. Tooth selection and preparation, type of attachment, unit of measurement, statistical analysis, and method of applying the debonding force (tensile versus shear), varies among studies. [40]

Differences in the direction of the application of force to cause bond failure, or the orthodontic attachment's position relative to the debonding force, can cause different stress patterns in the bracket-cement-enamel complex. [41] Variations in the point of force application and attachment choice has resulted in a wide spectrum of experimental results, which are often conflicting, and do not allow for comparison between studies. [42] Variations in the anatomy of the teeth result in different degrees of adaptation to the mesh pads on the bases of the curved brackets placed on the surface of the tooth. In a sense, it can be said that one size does not necessarily fit all. Furthermore, variation in the enamel

composition due to varying exposure to fluoride may affect the micro-mechanical bonding.

Variation in the size of the bonded area is directly proportional to the force required for failure. Variation in the force affecting the bracket due to inconsistent placement of the shearing knife or wire loop also affects failure measurements. To avoid these variations within and without the methods used in previous studies, the Single Plane Shear Test Assembly (SPSTA) [43, 44] was used. This technique was selected to limit the variables to those being studied.

b. Sample preparation

Bovine incisors were collected from Harris Beef Ranch in Selma, California. They were then gamma radiation-sterilized for infection control. [45] Soft tissue remnants were grossly removed from the root surfaces as seen in Figures 1 and 2.

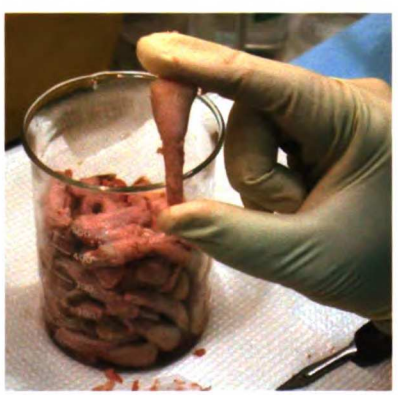

Figure 1. Harvested bovine incisors for use in sample preparation of 5x5 mm enamel blocks.

Figure 2. Soft tissue remnants were grossly removed from crown and root surfaces The teeth were gamma radiation-sterilized for infection control.

The crowns were sectioned from the roots using a hard-tissue saw (Buehler Isomet 11-1180 Low Speed Saw; Lake Bluff, IL) as viewed in Figure 3 on the following page. The facial surface was hemi-sectioned from the lingual surface. Three or four 5 x 5 x 2 mm blocks were harvested from each tooth's facial surface, depending on size and overall flatness of the parent tooth. The enamel surfaces of each block were flattened with 1200-grit silicon carbide sandpaper. Teeth with obvious enamel defects (cracks, chips, discoloration, demineralization, dentin perforation, or excessive curvature) were discarded. Ninety-six uniform 5 x 5 x 2 mm bovine blocks without visual defects were highly polished with sequential diamond abrasives of 6-µm, 3-µm, and 1-µm (Buehler Metadi Diamond Suspension In Water Base; Lake Bluff, IL) on a Buehler Ecomet II Polisher Grinder (Lake Bluff, IL) depicted in Figure 4 on the following page.

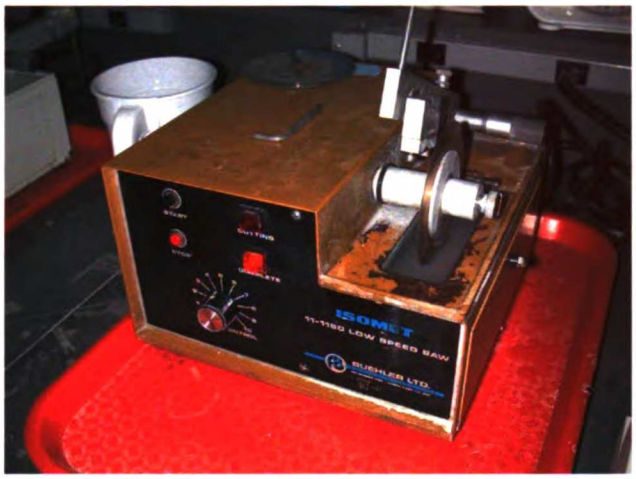

Figure 3. Buehler Isomet 11-1180 Low Speed Saw

Figure 4. Buehler Ecomet II Polisher Grinder with Buehler Diamond Abrasives

The bovine blocks, with reproducible enamel surfaces, were stored until use in a 100% humidity environment with 0.01% thymol in the water. Thirty-two of the ninety-six blocks were reserved for the present experiment.

Bovine tooth enamel has been shown to have similar results in adhesion tests with both composite resins and glass ionomer cements, when compared with human tooth enamel. [46-48] The adhesion to enamel and the superficial layer of dentin showed no statistically significant difference between human and bovine teeth, although the mean values were always slightly lower with bovine teeth. [47]

c. Laser parameters

A Q-switched Nd:YAG laser (New Wave Minilase III system; Sunnyvale, CA), operating at its third harmonic with a wavelength of 355 nm and a pulse duration (FWHM) of 5 ns, was used to irradiate the enamel surface of the bovine blocks.

Figure 5 depicts the laser set up used throughout this study. The Minilase III laser beam was focused onto the surfaces of the samples using BaF_2 and fused silica lenses (focal length 50 mm). A spot size (beam diameter) of 284 μm was produced by placing the lens 74 mm from the sample surface. A pyroelectric energy meter (Gentec Joulemeter ED-200; Ste. Foy, Quebec, Canada) was placed in the beam path behind the focusing stage to monitor and measure the beam energy to establish the beam profile.

The Gentec Joulemeter was connected to an oscilloscope (Tektronix TDS 210 Digital Real-time Oscilloscope; Beaverton, OR) for readout of total beam energy. Incremental adjustment of the beam energy yielded corresponding changes in fluence (measured in Joules/ cm^2). Increasing the beam intensity resulted in a similar rise in signal from the detector, as measured at the oscilloscope.

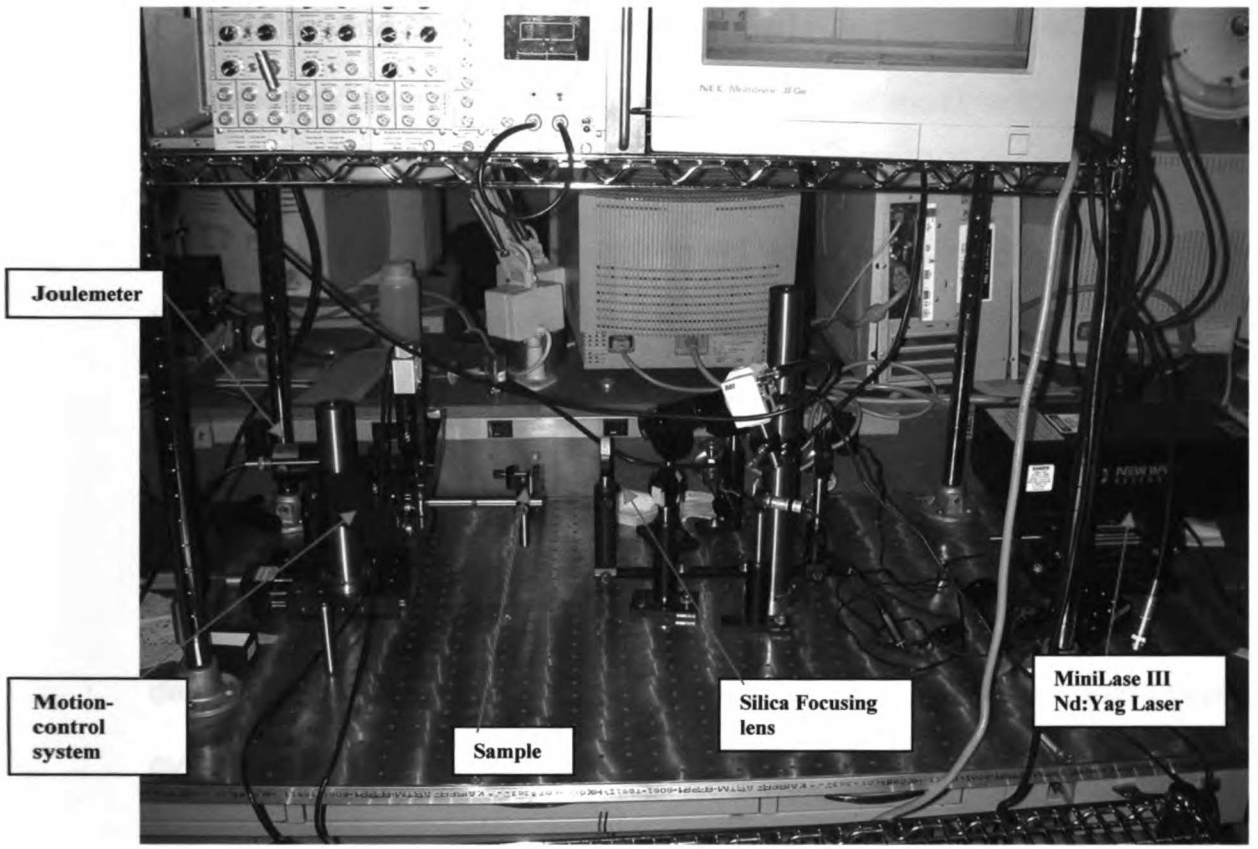

Figure 5. **Laser system set-up used throughout the study**

Four experimental sample groups were used (at fluences of approximately 2-, 4-, 6.5-, and 8 J/cm^2, *n*=8 each group). A pilot study of 3 samples was performed to determine the threshold for enamel modification and ablation. It was noted that the minimum fluence to cause a surface modification was 1.3 J/cm^2. These findings are in agreement with the 1.26 J/cm^2 fluence threshold level reported by Alexander. [49]

A beam profile was made to establish a 283-μm-diameter beam, which was used for sample irradiation. The beam were scanned across the 5 X 5 mm surface of each bovine block sample using the ESP3000 motion control system with an 850G actuator (Newport Electro-optics; Irvine, CA). Ten pulses were delivered for each spot with a scan distance of 100-μm between spots to provide overlap to more uniformly irradiate the surface. A repetition rate of 10 Hertz (Hz) was used for each sample, and each pulse had a duration of 5 nanoseconds (ns).

A representative sample from each group was assessed visually using an Olympus BX50 optical laboratory microscope (Melville, NY) with integrated DVC 1300C digital camera (Austin, TX) and Image Pro Plus ® software (Media Cybernetics, Silver Spring, MD). Digital images were captured at magnifications of 20x, 50x, 100x, and 200x.

d. Shear bond strength testing

To avoid disharmony between the curvature of the tooth surface and the curvature of the orthodontic attachment base, flat based orthodontic attachments

affixed to flattened enamel surfaces were used. In this method, a flat mesh-based rounded lingual button (Ormco® Flat Lingual Pad with Button Attachment; Glendora, CA) was selected. The advantage of a rounded attachment as opposed to a rectangular- or square-based attachment is the elimination of a sharp corner or projection that could be engaged prematurely or in an uneven fashion by the force delivery system. A misalignment of the bracket relative to the debonding force would cause the force to be directed at the projected corner thus altering the stress distribution that could prematurely debond the bracket. With a rounded attachment, the applied shearing force would always be tangential to the attachment base, regardless of the attachments orientation. By eliminating corners and projections, the application of the force becomes more predictable.

The force required to shear an orthodontic attachment from an enamel surface depends upon total bonded area. When a bonding agent is applied to a surface of a tooth it spreads unpredictably in all directions. The area it occupies depends upon the material used, the surface composition, tooth morphology, and the pressure on the attachment at the time of placement. In previous studies, investigators attempted to control this variable by applying a constant pressure during the bonding process, and by carefully removing the excess material "flash" with a sharp instrument. It is erroneous to assume that the total bonded area is the area underneath the bracket base. Uneven spread of the adhesive resin, presence of gaps or bubbles, and variation in the removal of the excess "flash" makes quantification of the bonded area impossible. It is common that during the

removal of excess resin adhesive by use of a sharp instrument, tear-out of bonding material from under the base occurs.

The necessity for a uniform and predictable bonding area was addressed by the use of an adhesive mylar strip. Using a sharp office hole-puncher, a 3.1 mm diameter hole was placed in the mylar strip. Using the adhesive side, the strip was then affixed to the surface of the prepared enamel surface, leaving a 3.1 mm diameter exposed space, depicted in Figure 6 on the following page.

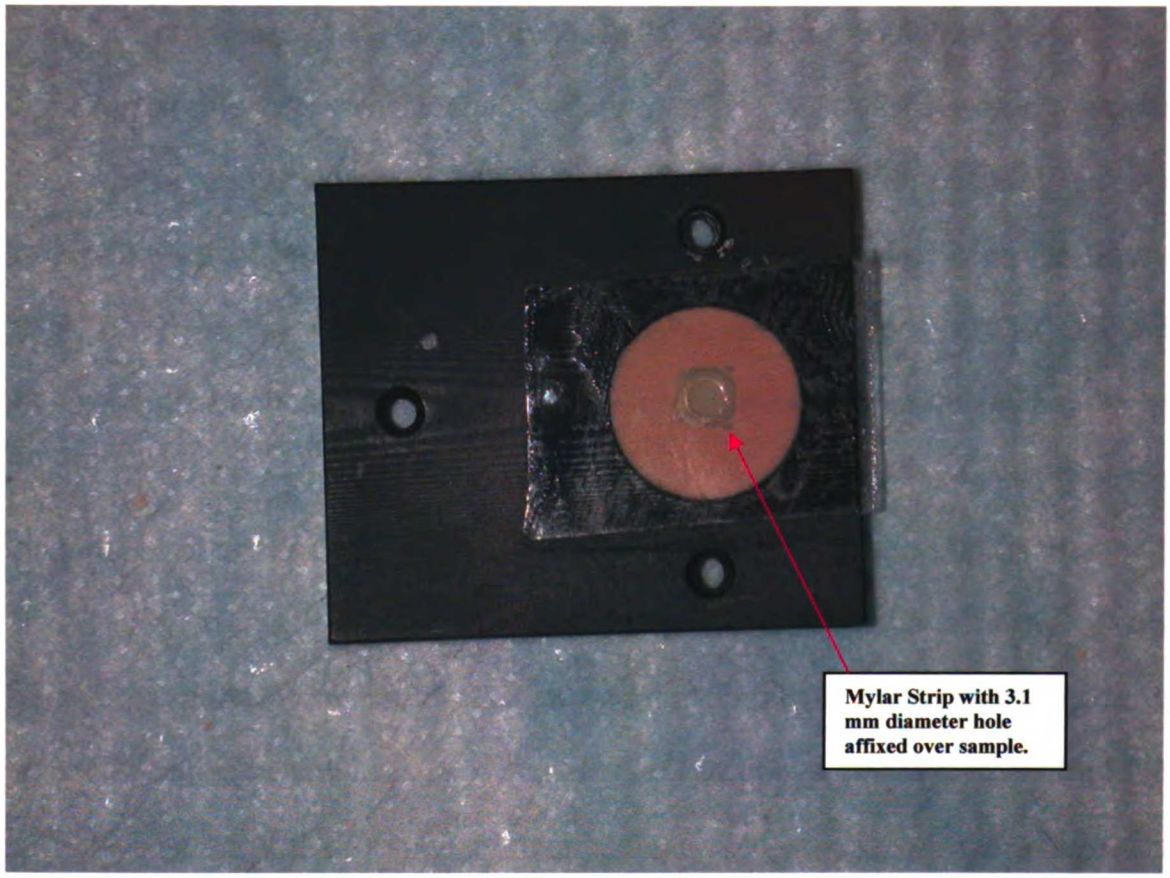

Figure 6. **Punctured adhesive mylar strip (3.1 mm hole) affixed over the sample imbedded in stone in Plate I.**

The orthodontic button used had a slightly larger diameter (3.25 mm) than the hole, and thus, when placed, completely covered the hole. A pilot study (n=4) was conducted to determine if the addition of an intervening mylar layer (of moderate thickness) between the tooth and the bracket would adversely affect bonding, and to determine if shear failure was an adhesive failure, a cohesive failure, or a combination adhesive-cohesive failure. An adhesive failure occurs between the tooth and the resin material. It is by far the most common failure type observed clinically and experimentally, and desired in the present experiment. A cohesive failure involves failure contained within the resin material itself or within the enamel. A cohesive failure simply notes the strength of the material or of the enamel in question and not its ability to bond with enamel. An excessively thick layer of bonding material could pre-dispose a failure at this level, and provide no useful clinical information about bond strengths. An adhesive-cohesive failure is a combination of the above where a fraction of the failure occurred at the tooth-resin interface and a fraction failed within the resin layer. A sample exhibiting a cohesive or adhesive-cohesive failure would be discarded and the use of the mylar strip method for controlling surface area invalid. All four sample types tested in the pilot study exhibited an adhesive-type failure.

To avoid the problems associated with shear tests using shearing knives or wire loops that produce shear-peel forces and not true shear forces, the modified single plane shear test assembly (SPSTA) was used. The SPSTA consists of two Delrin material plates. After the punctured mylar strip is placed on

the polished enamel surface, the sample block is affixed to Plate I with the tooth suspended through a countersunk funnel-shaped hole in the plate with dental die stone (Tuff Rock Formula 44 Synthetic Die stone [100 g powder: 20 cc H_20]; Brasilia, Brazil). The treated enamel surface is then flush with the shear plate.

The brackets were then bonded following manufacturer's directions to the exposed enamel through the hole in the mylar strip. The exposed bovine block surfaces were rinsed 20 seconds with water and dried completely with an air/water syringe. For the control group only (n=8), the surfaces were then prepared with 37% phosphoric acid for 30 seconds (Ormco Etchant Solution; Glendora, CA), and rinsed completely again for 30 seconds. (The 1.8-, 4.2-, 6.9-, 8.3- J/cm^2 laser treated samples were previously "etched" with the laser). The surfaces were re-dried and very thinly coated with an unfilled resin adhesive layer (3M Transbond XT Light Cure Adhesive Primer; 3M Unitek; Monrovia, CA). The mesh bases of the orthodontic buttons were coated with a filled composite resin (3M Transbond XT Light Cure Adhesive Paste; 3M Unitek; Monrovia, CA), and affixed to the prepared enamel surface. The buttons were held in piace by a weighted Gilmore needle (200 g) during the 40-second light curing process (Demetron Research Corporation Optilux Light Cure Unit @ 500 mw/cm^2; Danbury, CN) to control for dimension changes in the polymerization process. The result was an orthodontic attachment bonded to a bovine block affixed to a shear plate. The opposing member of the shear assembly (Plate II) was affixed to Plate I and held securely with 2 screws. Figure 7 shows that Plate II has a

smaller counter-sunk hole in which the protruding orthodontic attachment was housed.

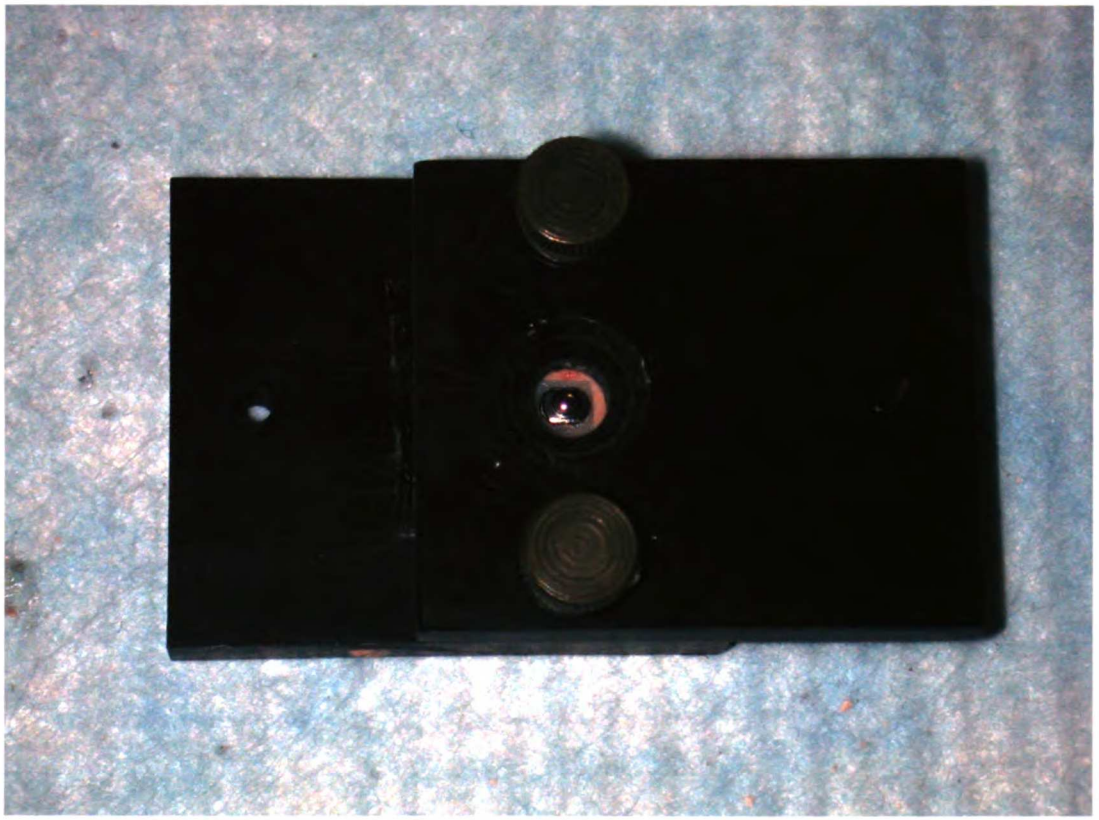

Figure 7. **Shear assembly (Plate II) was affixed to Plate I and held securely with 2 screws. Note the flat-based orthodontic attachment contained within the countersunk hole in Plate II.**

The countersunk hole was filled and condensed with multiple spills of Tytin amalgam (Kerr Corporation; Orange, CA), bonding the orthodontic attachment to Plate II. The SPSTA was then ready for shear testing.

The SPSTA was attached to an Instron tensile/shearing machine (Instron Model 1122 Electromechanical Test System; Canton, MA) with two aligning plates. The two screws holding the two members of the SPSTA were removed, leaving only the resin layer between the tooth and the attachment holding the plates together. The SPSTA, shown in Figure 8, allows the force of the machine to occur in one plane only, eliminating shear-peel effects.

Figure 8. **The single plane shear test assembly (SPSTA) affixed to the Instron Model 1122 Electromechanical Test System. Holding screws have been removed.**

The Instron Model 1122 Electro-mechanical tension and compression testing system, shown in Figure 9, was calibrated and set to record measurements in kilograms (Kg). A crosshead speed of 5 mm/min was used. The force level (measured in Kg) was recorded for each sample at the precise point when the two shear plates separated from each other. The recorded force-failure measurements were divided by the surface area of bonded region and multiplied by the conversion factor to convert the stress required for failure from Kg/cm^2 to Megapascals (MPa).

Figure 9. **Instron Model 1122 Electromechanical Test System**

e. Statistical analysis

The raw data from the shear bonding experiment (see appendix) were compiled and entered into a Microsoft Excell 2000 spreadsheet. Descriptive statistics (mean, standard deviation, and standard error of the mean) and inter-group analysis of variance (ANOVA) tests with the Scheffé Post-hoc correction were calculated with the StatView 5.0.1 software program package (SAS Institute, Inc., Cary, NC). All the samples were not truly independent because some came from the same teeth.

B. Specific Aim #2: Dissolution Rate Testing

a. Sample preparation and selection

Thirty-two of the original 96 blocks were set aside for this experiment. Sample fabrication followed the protocol previously described. The 32 samples were randomly assigned to each of the 4 experimental groups; n=8 each:

1) ***Untreated/non-irradiated group***
2) ***Laser only group***
3) ***Fluoride only***
4) ***Laser irradiated and fluoride treated group***

b. Laser treatment parameters

The laser parameters for the experiments for specific aim #2 were the same as in specific aim #1. The power output for the laser was set to provide a fluence of 2.5 J/cm^2 that was used for each of the laser-treated samples studied. This fluence was selected because it was well above the minimum threshold for enamel modification, but below the fluence levels that cause frank ablation and tissue loss. The fluence of 2.5 J/cm^2 also falls between 1.8 J/cm^2 mean fluence of group A, and the 4 J/cm^2 mean fluence from Group B from the bond strength experiments in Specific Aim 1.

c. Surface Dissolution

Seven liters of dissolution solution was made. Each liter of solution contained 7.456 grams of potassium chloride (0.1M KCl), 5.719 mL of concentrated glacial acetic acid (0.1M), and de-ionized water. Sodium hydroxide pellets and drops of 10% HCl were added as needed to titrate the pH to 4.500 $\pm$0.001. The TIM 900 Titration manager was calibrated and recalibrated (with pH 4 and pH 7 standards from Fisher Scientific; Hampton, NH) before use in determining the pH of the solution. A few drops of 0.01% thymol solution were added to the solution before being stored until used.

Each bovine block's base was affixed to a high-density polyethylene (HDPE) disc with ethyl cyanoacrylate adhesive (Krazy Glue, New York, NY). The sides of each sample were coated with 2 layers of an acid-resistant varnish, Revlon Nail Polish (New York, NY), to ensure that only the treated surface was exposed to the dissolution solution, shown in Figure 10.

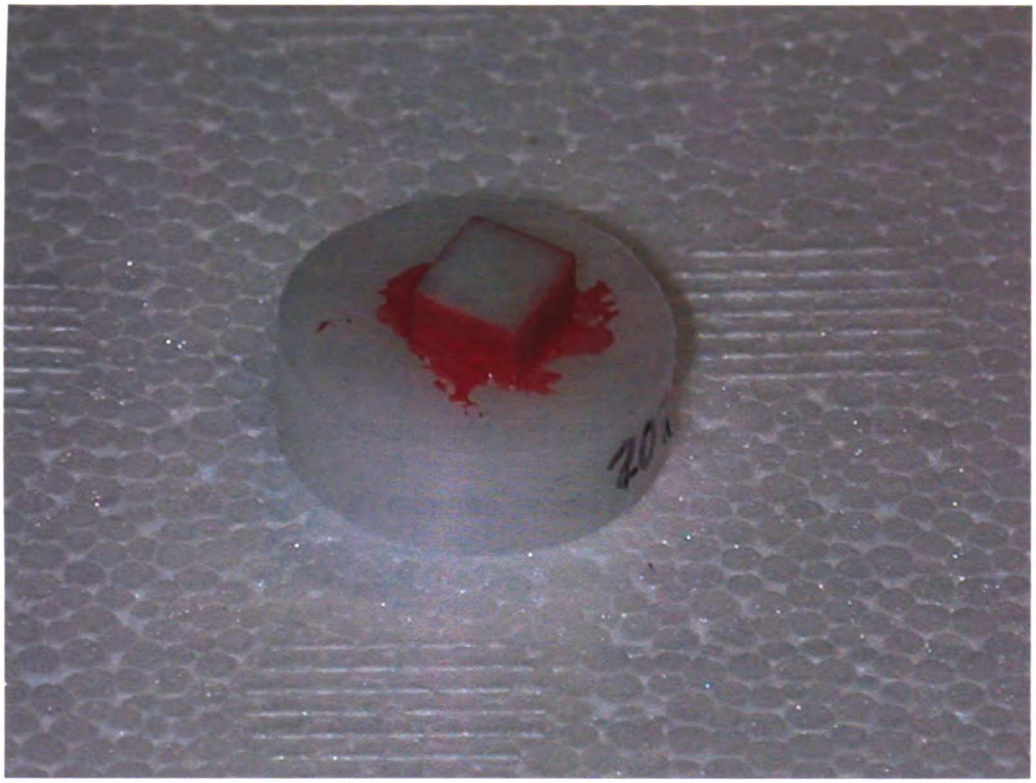

Figure 10. **Bovine block affixed to a high-density polyethylene (HDPE) disc. The sides of each sample were coated with 2 layers of an acid-resistant varnish. The blocks were placed in a stirring apparatus and placed in dissolution chamber for 20 minutes.**

Samples assigned to experimental groups 3 and 4 were given a one-time application of Sultan Topex 00:60-Second™ Fluoride Gel (1.23% Fluoride Ion APF; Englewood, NJ) prior to dissolution testing. Samples were given a 60 second application of fluoride gel, per manufacturer's directions, followed by a mild wash of de-ionized water to remove excess gel. Twelve cryogenic vials were prepared and used for each sample (where aliquots of the dissolution solution taken every 2 minutes, for 20 minutes, would be stored until analysis).

Two hundred milliliters of the dissolution solution was added to a Plexiglas dissolution chamber that was placed and warmed in a water bath maintained at 44 ° C. A 44 ° C water bath was used to expedite bringing room temperature solution to 37° C, without overheating the solution and thus affecting dissolution rates. Once the dissolution solution in the chamber was warmed to 37 ° C, the HDPE discs were affixed to a holder, placed into the chamber, and the stirring apparatus turned on (300 RPM $\pm$ 20) thus beginning the dissolution process. (The temperature within the chamber never increased greater than 0.5 ° C during the course of the dissolution). A steady stream of nitrogen gas was bubbled through the solution during each experiment. Two milliliters of the solution were withdrawn every 2 minutes and placed in the appropriate cryogenic vial and stored for subsequent calcium and phosphate analysis.

d. Phosphate analysis using UV spectrophotometry

Phosphate standard solutions of 0-, 0.25-, 0.5-, 1- and 2-parts per million phosphate (as phosphorus), and samples from demineralization solutions were prepared with Reagent C. Two hundred-fifty milliliters of Reagent C was prepared containing 100 ml of de-ionized water, 50 ml 6N H_2SO_4, 50 ml 2.5% ammonium molybdate, and 50 ml of 10% ascorbic acid. Phosphorus and ammonium molybdate form a colored complex that absorbs light at a wavelength of 820 nm. The Genesys 5 UV Spectrophotometer ThermoSpectronic: Rochester, NY) operating at a wavelength of 820 nm, was used to analyze and quantify the concentration of phosphate from the phosphate standards and experimental samples. The values were read in absorption units. Multiple readings were made for each aliquot. The values for each sample were averaged, multiplied by the dilution factor, and divided by the absorption unit reading for the 1-ppm phosphate (as phosphorus) standard (0.447) to yield the concentration of phosphate in ppm (as phosphorus) for each time point for each sample. The values were plotted and graphed using Igor Pro 4.01 software by Wavemetrics (Lake Oswego, OR). A linear dissolution plot was recorded for each, and its slope measured and recorded for subsequent statistical analysis.

e. Calcium Analysis using atomic absorption (AA) spectrophotometry

Standard solutions of 0.5-, 1.0-, 2.0-, and 5.0-ppm calcium were prepared by diluting the 1000-ppm calcium standard solution with 1000-ppm potassium chloride (KCl) solution. These standards were used to calibrate the Perkin Elmer 3110 Atomic Absorption (AA) Spectrophotometer (Wellesley, MA). The potassium reduces ionization of the calcium, as the potassium freely ionizes preferentially over the calcium. Elemental calcium is necessary for the specific wavelength absorption of AA. Samples of the demineralization solutions (1 ml) were diluted 10 times with KCl solution. This mixture was passed through the air/acetylene/N_2O flame and analyzed with AA. Sample values were multiplied by the sample dilution factor to calculate the concentration of calcium in ppm. The values were plotted and graphed using Igor Pro 4.01 software by Wavemetrics (Lake Oswego, OR). A linear dissolution plot was recorded for each, and its slope measured and recorded for subsequent statistical analysis.

f. Statistical analysis

The raw data from the calcium and phosphate analyses (see appendix) were compiled and entered into a Microsoft Excel 2000 spreadsheet. Descriptive statistics (mean, standard deviation, and standard error of the mean) and inter-group analysis of variance (ANOVA) tests with the Sheffé Post-hoc correction

were calculated and tabulated with the StatView 5.0.1 software program package (SAS Institute, Inc., Cary, NC).

C. Specific Aim #3: Microscopic and Chemical Analysis

a. Rationale

To verify that the mineral components of the enamel tissue were not altered chemically under the process of laser irradiation, it was necessary to take infrared absorption spectra from several samples representative of those used in the aforementioned experiments, as well as others covering a continuum of fluences from sub-threshold levels to very high levels, and compare those spectra to those obtained from non-irradiated, highly-polished bovine block controls. A change in spectra from the untreated control to laser treated sample would indicate a chemical change in the mineral matrix. Mineral components under certain laser systems and conditions exhibit the transformation of hydroxyl- and carbonated-apatite to more soluble and weaker calcium phosphate phases. Weak phases of calcium phosphate may result in de-lamination and cavitation of the treated surface resulting in frank tissue loss, poor acid challenge resistance, and poor bond strengths. It is of utmost concern that, at minimum, the treatments performed on the teeth through laser irradiation leave the enamel mineral in its original crystal structure.

b. Fourier Transform Infrared (FTIR) analysis

Two infrared spectrometers were used to obtain spectra. The RFX-30 FTIR spectrometer (Laser Precision Analytical; Irvine, CA) was used in a pilot study analysis of a few treated and untreated samples (n=4). Figure 11 shows the Nicolet Magna 760 Nic-Plan IR Microscope (Madison, WI) at the Advanced Light Source Laboratory at the Ernest Orlando Lawrence Berkeley National Laboratory; Berkeley, CA, that was used to achieve very high resolution, accurate infrared spectra from representative samples from each treatment group.

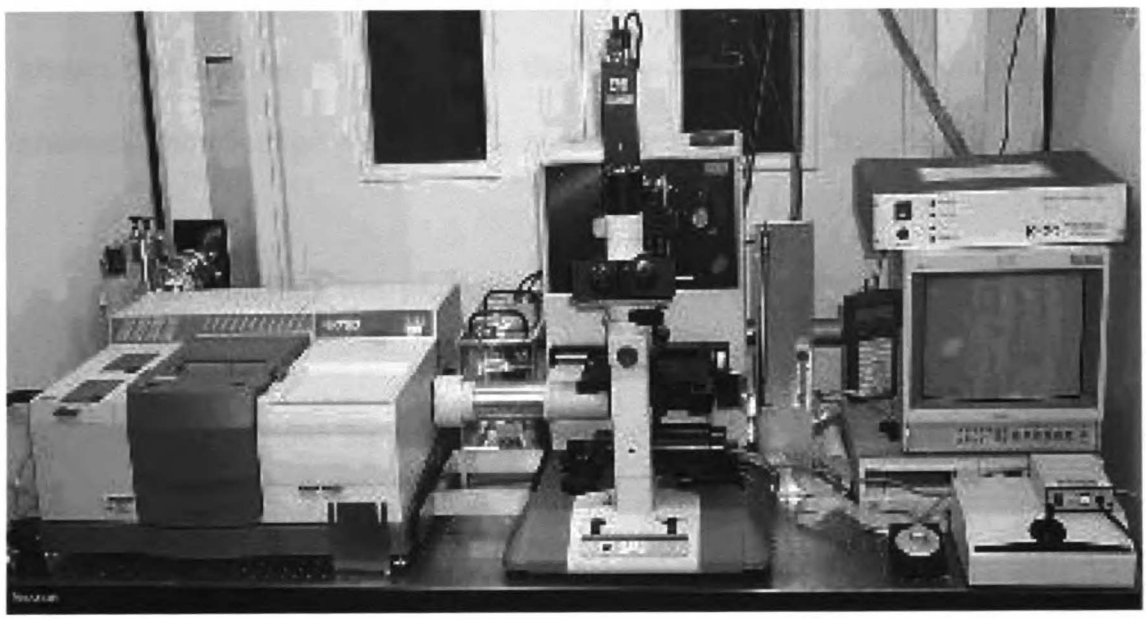

Figure 11. **Nicolet Magna 760 Nic-Plan IR Microscope.**

An additional sample, irradiated at 1 J/cm^2 with the Argus CO_2 laser (λ = 9.6-μm, 5-8 μs pulse duration) was also included as an additional control. It is known that enamel, irradiated with the Argus CO_2 (λ = 9.6-μm), undergoes slight chemical modification with the loss or reduction of the carbonate. [6, 8]

c. Surface morphology analysis using SEM

Representative samples from each of the treatment groups studied in the experiments in Specific aims #1 and #2 (containing samples treated under 5 different laser conditions, and samples etched with conventional 37% ortho-phosphoric acid, and untreated controls) were gold surface-sputtered following established protocols and imaged with the Topcon SX-40A "wet" SEM with CFAS (Topcon Instruments, Pleasanton, CA) at 30x, 300x, 1000x, and 2000x magnifications, shown in Figure 12 on the following page.

Images were captured and stored in digital format. A sub-group of samples that were used in the shear bond strength tests were cross-sectioned and polished (same protocol as previously described through 1-μm diamond slurry) to view the resin-enamel interface. All images were cataloged for subsequent descriptive analysis of the imaged surfaces.

Figure 12. **Topcon SX-40A "wet" environmental SEM**

V. RESULTS

A. Specific Aim #1: Shear Bond Strength Testing

a. Shear Bond Strength Testing

Modification of the enamel surface was performed using 5 nanosecond pulses from the Nd:YAG laser operating with a wavelength in its third harmonic (355 nm), as described in the materials and method section. Table 1 displays the mean shear bond strengths, listed in decreasing order and measured in Megapascals (MPa), for each of the four laser-irradiated treatment groups, the one positive (acid-etched) control group, and the one negative (untreated) control group. The mean fluences (measured in J/cm^2) for each laser-treated subgroups are also noted.

Mean Fluence	Treatment Group	*n*	Mean Bond Strength	*sd*	Statistical Significance*
	Positive Controls *(30 second etch with 37% phosphoric acid)*	9	***29.5 MPa***	1.9	**A**
6.9 J/cm2	**Moderate-High Fluence**	8	***20.7 MPa***	1.7	**B**
8.3 J/cm2	**High Fluence**	8	***20.4 MPa***	2.1	**B**
4.2 J/cm2	**Moderate Fluence**	8	***17.2 MPa***	1.5	**C**
1.8 J/cm2	**Low Fluence**	7	***16.7 MPa***	2.7	**C**
	Negative Controls *(Direct bonding to unetched/untreated enamel)*	3	***1.1 Mpa***	0.2	**D**

Table 1. **Mean shear bond strengths (MPa) with standard deviations for each of the six treatment groups. The mean fluences (measured in J/cm^2) for each laser-treated subgroup are also noted.**

*** Groups with the same letter are not significantly different ($p < 0.05$) by ANOVA and Sheffé post-hoc test**

Statistically significant differences between treatment groups were determined with ANOVA statistical testing utilizing the conservative Scheffé post-hoc test (Significance level: $p< 0.05$). The only *non*-significant differences that were observed were between the low and moderate fluence groups and the moderate-high and high fluence groups.

A small sample size (n=3) was required to demonstrate the negligible shear bond strengths of composite resin to untreated, highly polished enamel for the negative control group. Mean shear bond strengths were not only extremely low, but also consistent enough to characterize this group. One sample, shown in Figure 13, from the low fluence group was omitted because the bond failure occurred partly within the resin layer, and partly between the resin and the mesh base of the attachment as demonstrated in the SEM micrograph below.

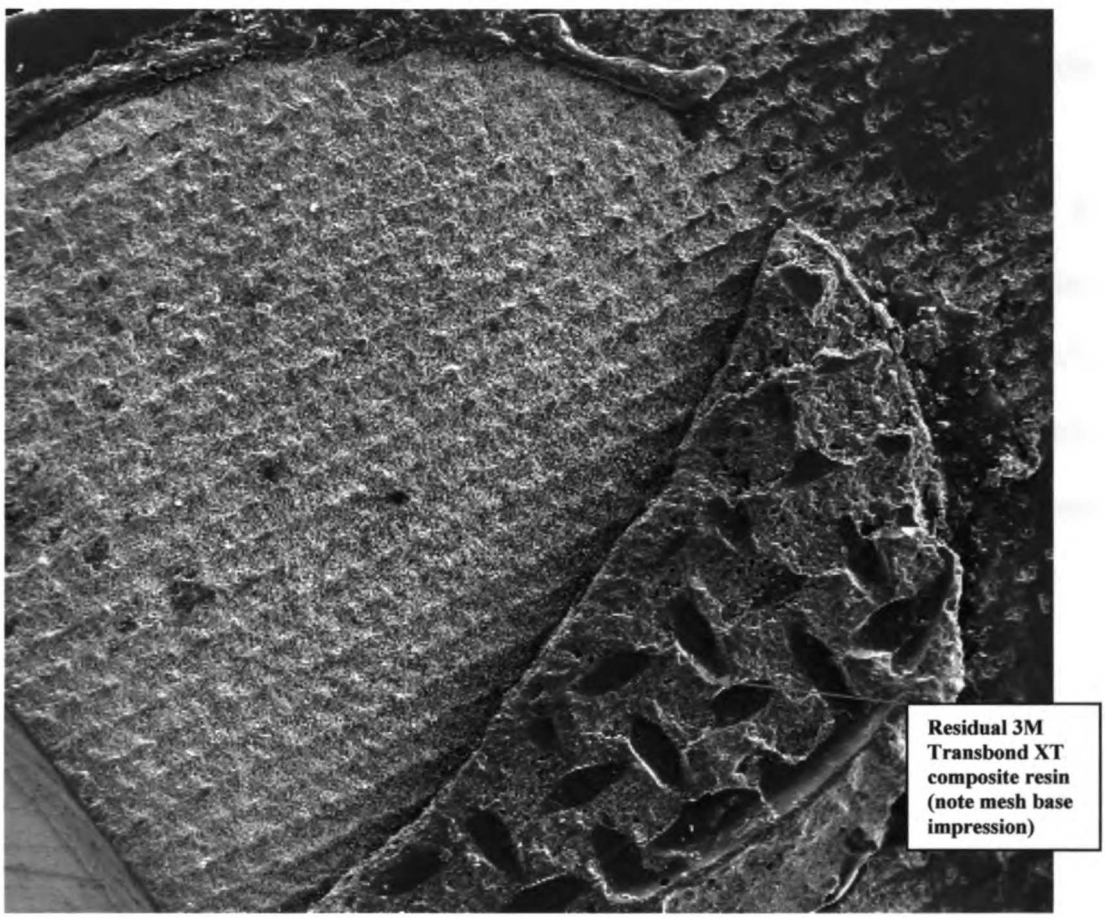

Figure 13. **SEM image (70x magnification) showing residual composite (3M Transbond XT) after shear–bond testing. This sample was discarded from bonding study because partial bond failure occurred between the mesh base of the attachment and the composite resin. Orthodontic attachment is 3.1 mm in diameter.**

All laser-irradiated bovine block samples had shear bond strengths higher than non-treated, non-etched negative controls. The data is depicted graphically in Figure 14 on the following page. However, the samples etched for 30 seconds with the 37% ortho-phosphoric acid had consistent and statistically significant ($p < 0.05$) higher bond strengths than those of the laser-irradiated blocks. It should be noted, however, that even the low fluence group (1.8 J/cm^2), with mean group fluence slightly above the modification threshold fluence (1.3 J/cm^2) produced relatively high shear bond strength. The mean shear bond strength for the low fluence group approximates shear bond strengths reported for resin reinforced glass ionomer-bonded samples (12-20 MPa). [50] ,[51]

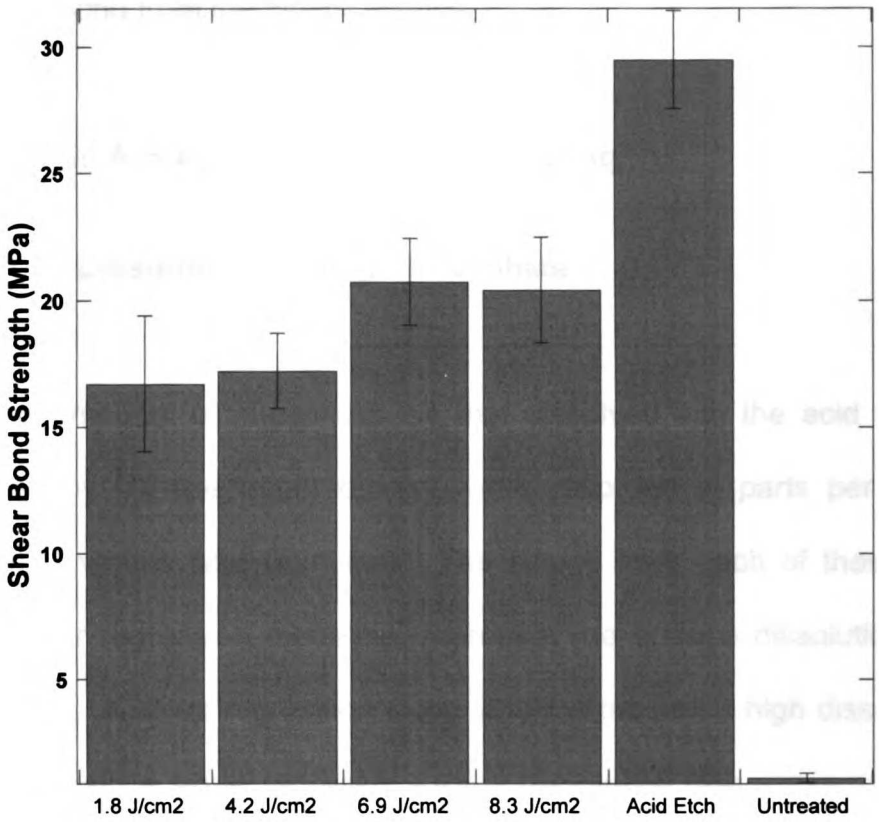

Figure 14. **Mean shear bond strengths, with standard deviation error bars, for each of the 6 treatment groups. High shear bond strengths (*29.5 MPa*) were recoded with conventional acid etching. The low fluence group (1.8 J/cm^2), with mean group fluence slightly above the modification threshold fluence (1.3 J/cm^2) produced relatively high shear bond strengths. A large increase in fluence yielded only a mild increase in shear bond strengths.**

As expected, negligible bond strengths were achieved when resin was applied to unetched, untreated negative control samples. As mentioned previously, fluences just above threshold were able to create a substantial increase in shear bond strength compared to the negative control. However, an increase in fluence from 1.8 to 8.3 J/cm^2 yielded approximately only a 4 MPa increase in shear bond strength. While statistically significant, these slight

increases in shear bond strengths may not be clinically worth the extent of ablation resulting from the higher fluence.

B. Specific Aim #2: Dissolution Rate Testing

a. Dissolution Testing: Phosphate

The amounts of phosphate ion that dissolved into the acid solution, as determined by UV-spectrophotometry, were recorded in parts per million (as phosphorus) versus time (minutes). The slopes from each of these samples, utilizing linear regression modeling, represent the surface dissolution rates for each sample. A steep regression slope would represent a high dissolution rate, while a flatter slope would represent a lower dissolution rate.

Table 2 on the following page shows phosphate dissolution rates (mg/L/minute phosphorus) for each of the samples evaluated. The average percentage of inhibition for each treatment group, as compared to the control group, is also shown.

CONTROL	SLOPE	AVERAGE	SD	% INHIBIT	*Statistical Significance
201	0.0224				
202	0.0159				
203	0.0158				
204	0.0224	0.0192	0.0036	0%	A
205	0.0216				
206	0.0219				
207	0.0144				

LASER	SLOPE	AVERAGE	SD	% INHIBIT	*Statistical Significance
A	0.0245				
B	0.0247				
C	0.02				
D	0.0261	0.0223	0.0046	-16%	A
E	0.0245				
F	0.0122				
G	0.0205				
H	0.0255				

FLUORIDE	SLOPE	AVERAGE	SD	% INHIBIT	*Statistical Significance
I	0.0117				
J	0.0216				
K	0.00224				
L	0.0196	0.0181	0.0041	6%	A
M	0.0117				
N	0.0189				
O	0.0189				
P	0.02				

LASER/FLUORIDE	SLOPE	AVERAGE	SD	% INHIBIT	*Statistical Significance
Q	0.00688				
R	0.0214				
S	0.00361				
T	0.00648	0.0089	0.0058	54%	B
U	0.00575				
V	0.00714				
W	0.0136				
X	0.00633				

Table 2. The amounts of phosphate ion (as phosphorus) that dissolved into the acid solution, as determined by UV- spectrophotometry, were recorded in parts per million versus time (minutes). The slopes, noted above, represent the surface dissolution rates for each sample. The laser and fluoride treated group exhibited a 54% increase in dissolution resistance.

*Values with same letter are not significantly different ($p < 0.05$) by ANOVA and Sheffé post-hoc test.

The results clearly show that the combination treatment of laser irradiation (fluence of 2.5 J/cm^2) and one-time fluoride application considerably reduced the extent of the dissolution of phosphate from the enamel surface. Statistically significant differences between treatment groups were noted with ANOVA statistical testing utilizing the conservative Sheffé post-hoc test (significance level: $p < 0.05$).

Neither the laser alone group, nor the fluoride alone group, significantly increased the resistance to acid dissolution. The laser treatment followed by a topical application of fluoride increased the resistance to acid dissolution by 54% over controls. The only statistically significant differences noted were between the laser and fluoride treatment group and each of the other experimental groups.

Fluoride application to polished bovine enamel resulted in a non-significant, apparent 6% improvement in dissolution resistance versus the control. Laser irradiation (fluence = 2.5 J/cm^2) seemed to increase the degree of dissolution compared to control samples (addressed in the Discussion section), but the difference was not significant. However, the combination of laser irradiation and one-time fluoride application yielded a synergistic effect by vastly reducing dissolution rates by 54%, as compared to control ($p < 0.05$).

The mean dissolutions of phosphate in parts per million (ppm as phosphorus) for each treatment group are illustrated in Figure 15.

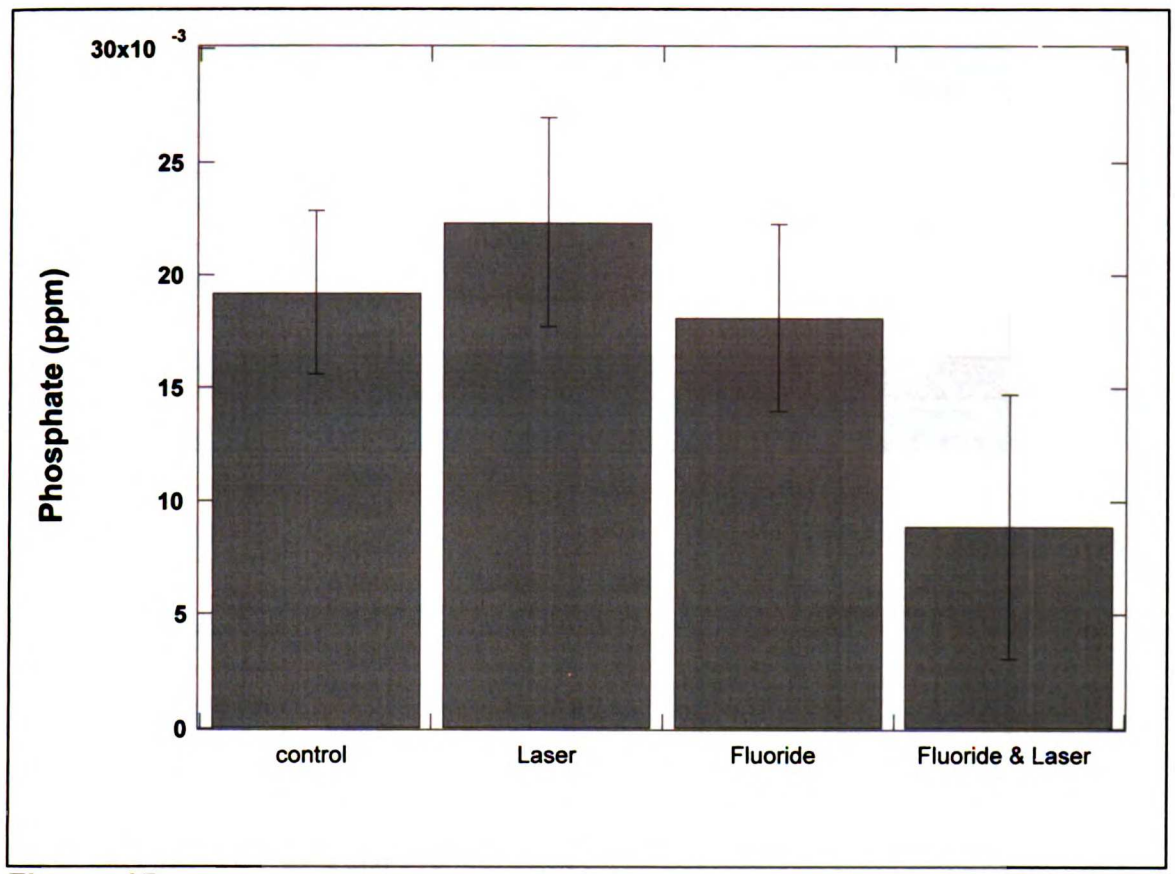

Figure 15. **The mean dissolutions of phosphate (as phosphorus) in parts-per-million (ppm) for each treatment group. Fluoride & laser group was significantly different from the other treatment groups.**

b. Dissolution Testing: Calcium

The amount of calcium ions that dissolved into the acid solution, as determined by atomic absorption (AA) spectrophotmetry, were recorded in parts per million (ppm calcium) versus time (minutes). The slopes from each of these samples, obtained through linear regression modeling, represents the surface dissolution rates (mg/L/minute calcium) for each sample. The slopes for each sample are recorded in Table 3. The average percentage of inhibition for each treatment group, as compared to the control group, is also shown.

CONTROL	SLOPE	AVERAGE	SD	% INHIBIT	*Statistical Significance
201	0.0496				
202	0.0381				
203	0.0349				
204	0.0504	0.0419	0.0087	0%	A
205	0.0487				
206	0.044				
207	0.0275				

LASER	SLOPE	AVERAGE	SD	% INHIBIT	*Statistical Significance
A	0.056				
B	0.0554				
C	0.0434				
D	0.0648	0.0489	0.012	-16 %	A
E	0.0488				
F	0.0244				
G	0.0427				
H	0.0556				

FLUORIDE	SLOPE	AVERAGE	SD	% INHIBIT	*Statistical Significance
I	0.0257				
J	0.0499				
K	0.0487				
L	0.0457	0.0374	0.011	10%	A
M	0.0287				
N	0.0418				
O	0.0208				
P	0.0378				

LASER/FLUORIDE	SLOPE	AVERAGE	SD	% INHIBIT	*Statistical Significance
Q	0.0178				
R	0.0431				
S	0.00877				
T	0.0143	0.0198	0.011	53%	B
U	0.013				
V	0.0164				
W	0.031				
X	0.014				

Table 3. The amounts of calcium ion that dissolved into the acid solution, as determined by Atomic absorption spectrophotometry, were recorded in parts per million versus time (minutes). The slopes, noted above, represent the surface dissolution rates for each sample. The laser and fluoride treated group exhibited a 53% increase in dissolution resistance.

*Values with same letter are not significantly different ($p < 0.05$) by ANOVA and Sheffé post-hoc test.

The results clearly show that the combination treatment of laser irradiation (fluence of 2.5 J/cm^2) and one-time fluoride application considerably reduced the extent of the dissolution of calcium from the enamel surface. Statistically significant differences between treatment groups were noted with ANOVA statistical testing utilizing the conservative Scheffé post-hoc test (significance level $p < 0.05$). The statistical results are identical, as expected, with those in the phosphate analysis.

Neither the laser alone group, nor the fluoride alone group, significantly increased the resistance to acid dissolution. The laser treatment followed by a topical application of fluoride increased the resistance to acid dissolution by 53% over controls. The only statistically significant differences noted were between the laser and fluoride treatment group and each of the other experimental groups.

The calcium analysis was used to confirm and support the findings from the phosphate analysis. No major discrepancies between the calcium and phosphate analyses were noted. The fluoride treatment group in the phosphate analysis exhibited a 6% inhibition, while a 10% inhibition was observed in the calcium analysis.

As expected, there was approximately a two-fold higher (2.17x) concentration of calcium than of phosphate (as phosphorus). See Appendix. The results depicted in Figure 16 on the following page clearly show that the combination treatment of laser irradiation (fluence of 2.5 J/cm^2) and one-time

fluoride application considerably reduced the extent of the dissolution of calcium from the enamel surface.

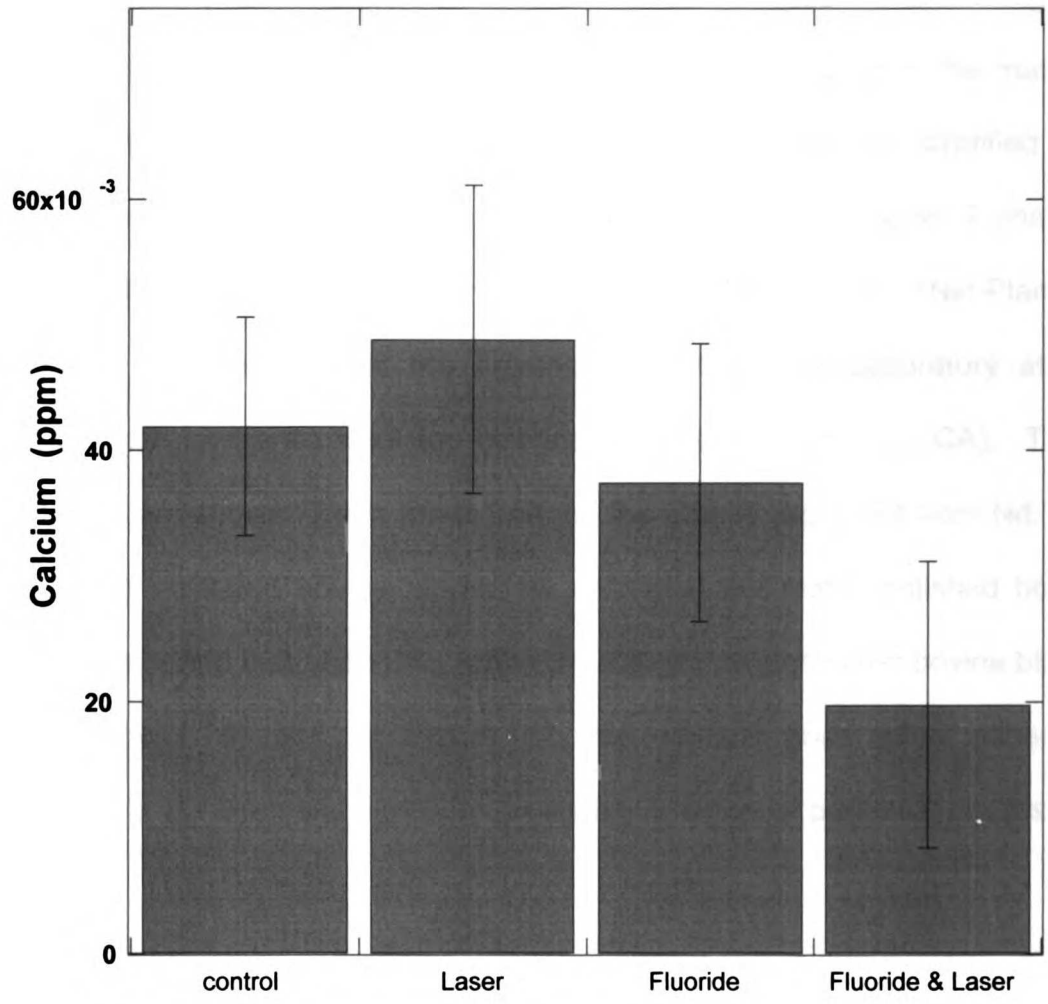

Figure 16. **The mean dissolution of calcium in parts-per-million (ppm) for each treatment group. Fluoride & laser group significantly different from other treatment groups.**

C. Specific Aim #3: Microscopic and Chemical Analysis

a. Fourier Transform Infrared Analysis

The effects of irradiation of bovine enamel surfaces were investigated using 355 nm laser pulses according to protocols as discussed in the material and methods section. The following figure shows the spectra, stratified and separated for visual clarity, of three spectra generated from a Fourier Transform Infrared (FTIR) spectrophotometer (The Nicolet Magna 760 Nic-Plan IR Microscope (Madison, WI) at the Advanced Light Source Laboratory at the Ernest Orlando Lawrence Berkeley National Laboratory; Berkeley, CA). Three distinct plots are shown. From top to bottom, the graphs represent from Nd:YAG (λ= 355 nm) irradiated bovine blocks; an untreated but highly polished bovine block (control) ; and that of an CO_2 Argus (λ= 9.6-μm) laser-treated bovine block.

On the FTIR plot, in Figure 17, two vertical lines were added at approximately 1475-μm and 1340-μm, to denote a region of particular interest.

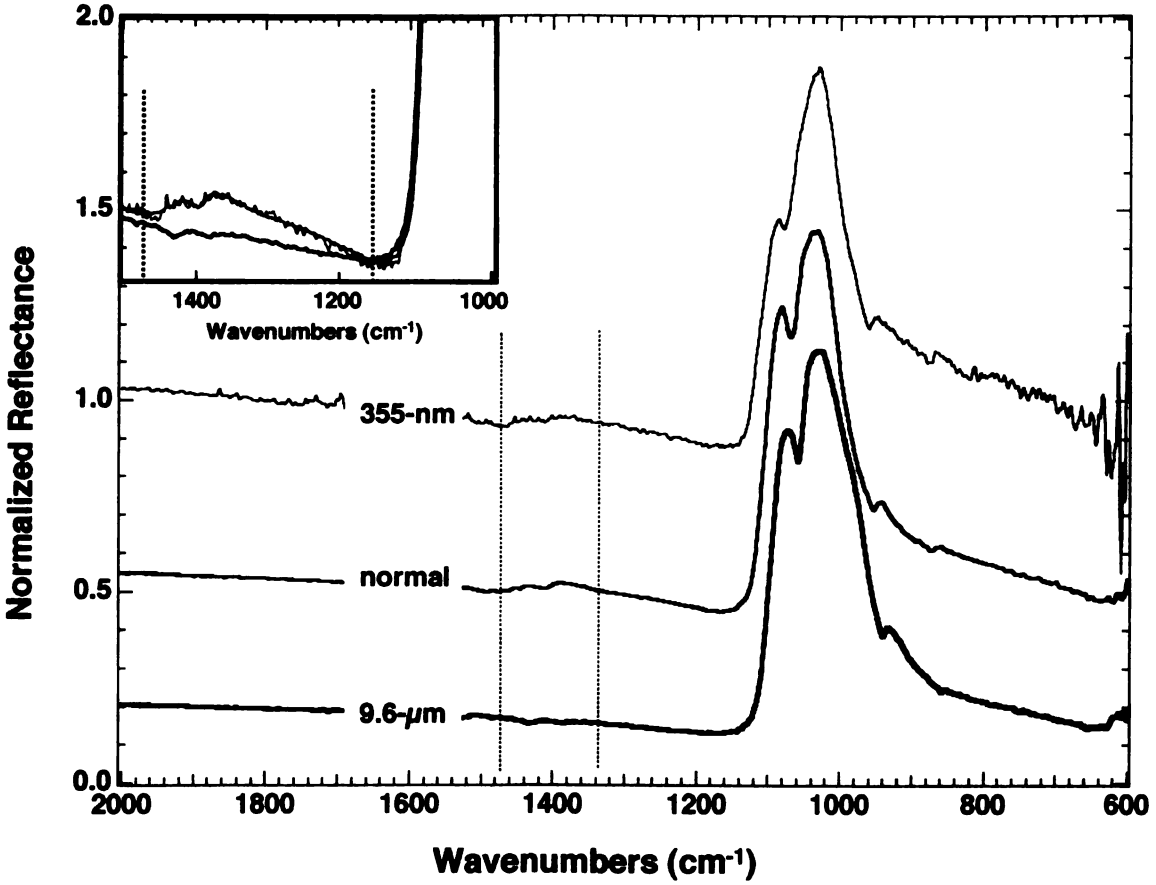

Figure 17. FTIR Spectra. From top to bottom (separated for clarity), the spectra are from a λ=355 nm laser irradiated sample, an untreated control sample, and a CO_2 irradiated (9.6-μm) sample. A subtle carbonate peak can be located in the region bounded by two vertical lines for both the control and λ=355 nm laser irradiated samples. The inset shows a magnified view of the superimposed carbonate peaks for each of three groups. Note: the Nd:YAG treated sample's plot has a slight increase in "noise", secondary to the surface roughness.

The untreated control sample and the Nd:YAG laser irradiated (355 nm) sample both share a subtle peak bounded by the aforementioned lines. The presence of this peak indicates the normal presence of carbonate within the mineral substance. The Argus CO_2 (λ= 9.6-μm) laser-irradiated sample does not have this peak, [52, 53] suggesting that the CO_2 laser modifies and alters the chemical structure of enamel when irradiated. On the other hand, the Nd:YAG laser,

operating at 355 nm, does *not* modify the normal chemical structure of enamel mineral, having a spectrum identical to non-irradiated, pristine enamel. The presence of the carbonate peak was observed in each of the Nd:YAG-irradiated samples tested, covering a spectrum of fluences from 1.3 J/cm^2 to 9.5 J/cm^2. In essence, the beam wavelength served as the determinant for the chemical modification of the enamel, and not the beam intensity (fluence).

b. Scanning Electron Microscopy—Morphological evaluation

Scanning electron micrographs of highly polished, untreated bovine enamel (Figure 18A) and Nd:YAG (λ = 355 nm) laser treated enamel (Figure 18B) are shown below at 700x and 300x magnification, respectively. Note the uniformly modified and roughened surface achieved by using a highly accurate motion control stage. Light optical photographs taken at a 200x magnification are also shown for comparison in Figure 18C and Figure 18D below. Note superficial craze lines in the non-irradiated sample in Figure 18. The presence of craze lines is a normal variant in enamel anatomy and not specifically induced under laser irradiation.

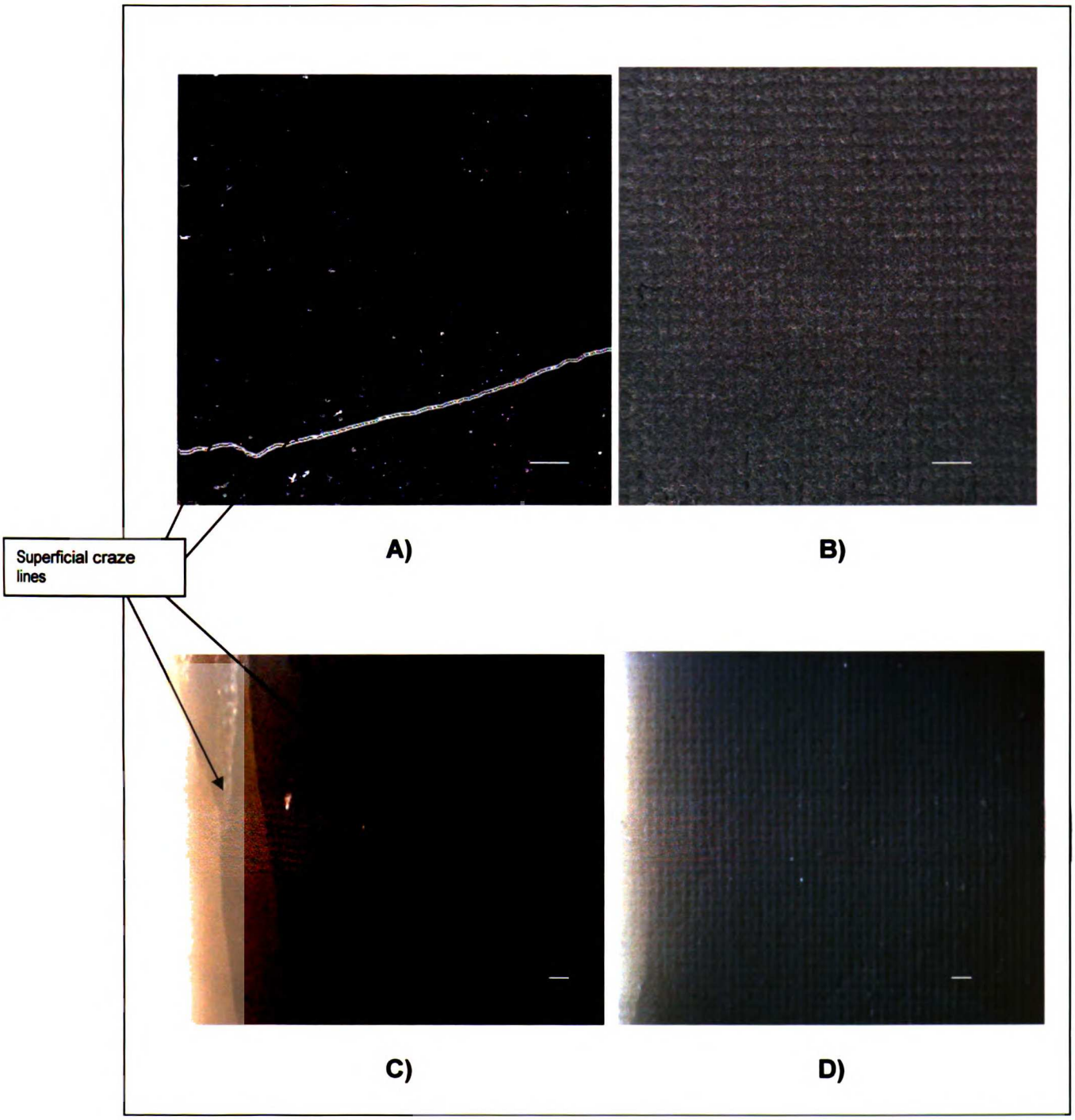

Figure 18. **SEM micrographs of A) Highly-polished bovine block (300X Magnification) and B) Laser-irradiated bovine block (4.5 J/cm2; 300x magnification) are shown.**
Light optical photographs of C) Highly-polished bovine block (200X magnification) and D) Laser-irradiated bovine block (4.5 J/cm2; 200x Magnification) are shown. Note the presence of natural craze lines in untreated bovine enamel (arrows) in A) and C). Bar= 200 micrometers.

At higher magnification, it becomes clear that the ablation was a clean process without evidence of charring or micro fracturing of adjacent, non-irradiated enamel tissue. Figure 19 clearly demonstrates the presence of intact enamel rods (of 4- to 5-µm width) with the inter-prismatic tissue selectively removed (1,000x magnification; fluence 2.5 J/cm^2).

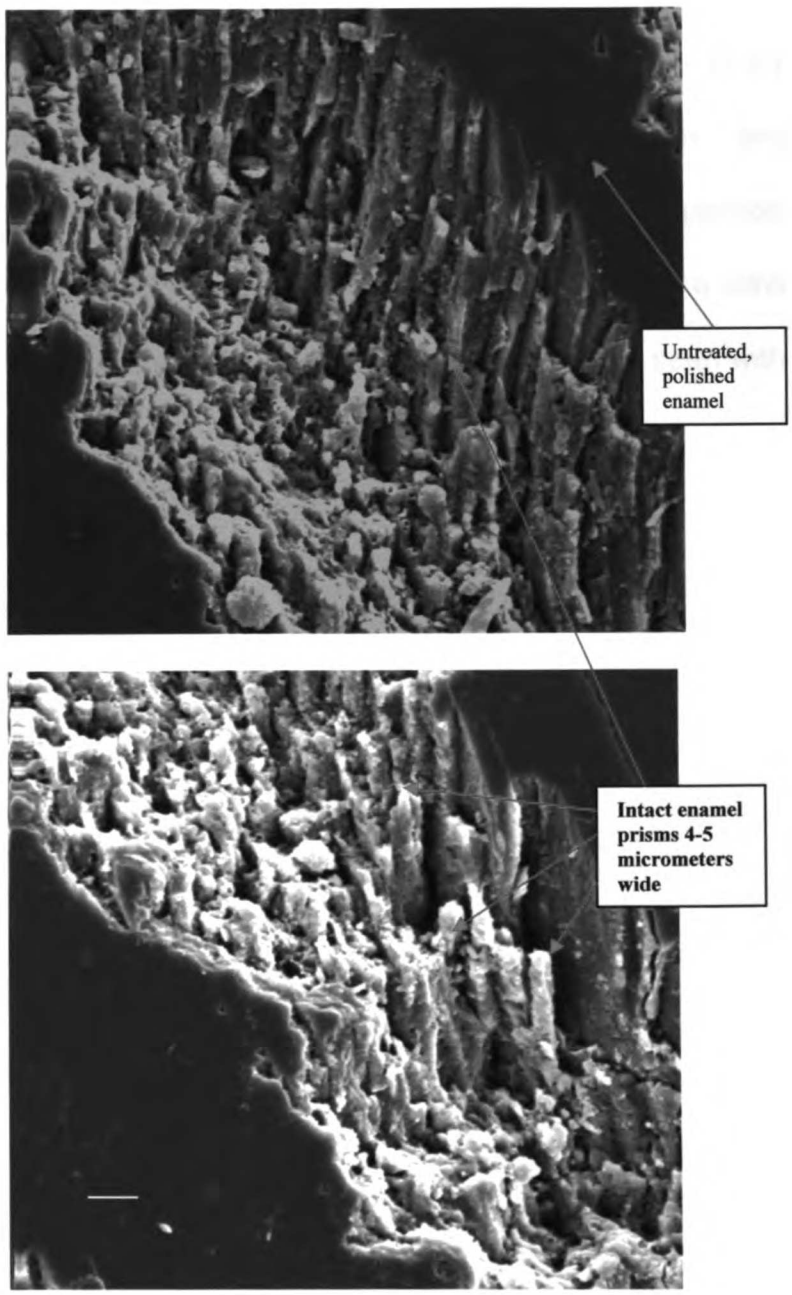

Figure 19. **SEM micrographs (1000x magnification) of two separate laser-irradiated samples A) and B) (fluence 2.5 J/cm^2) clearly show presence of intact enamel rods (of 4- to 5-µm width) with the inter-prismatic tissue selectively removed. Bar= 10 µm.**

Figure 20, on the following page, shows a similar pattern of modification clearly demonstrating the presence of intact enamel rods (of 4- to 5-μm width) with the inter-prismatic tissue selectively removed (300x and 1,000x magnification). The samples were irradiated with a fluence of approximately 4.2 J/cm^2. Figure 21 further exhibits the ability laser-irradiation with a wavelength of 355 nm to selectively modify the surface of bovine enamel, as seen with a slightly higher magnification..

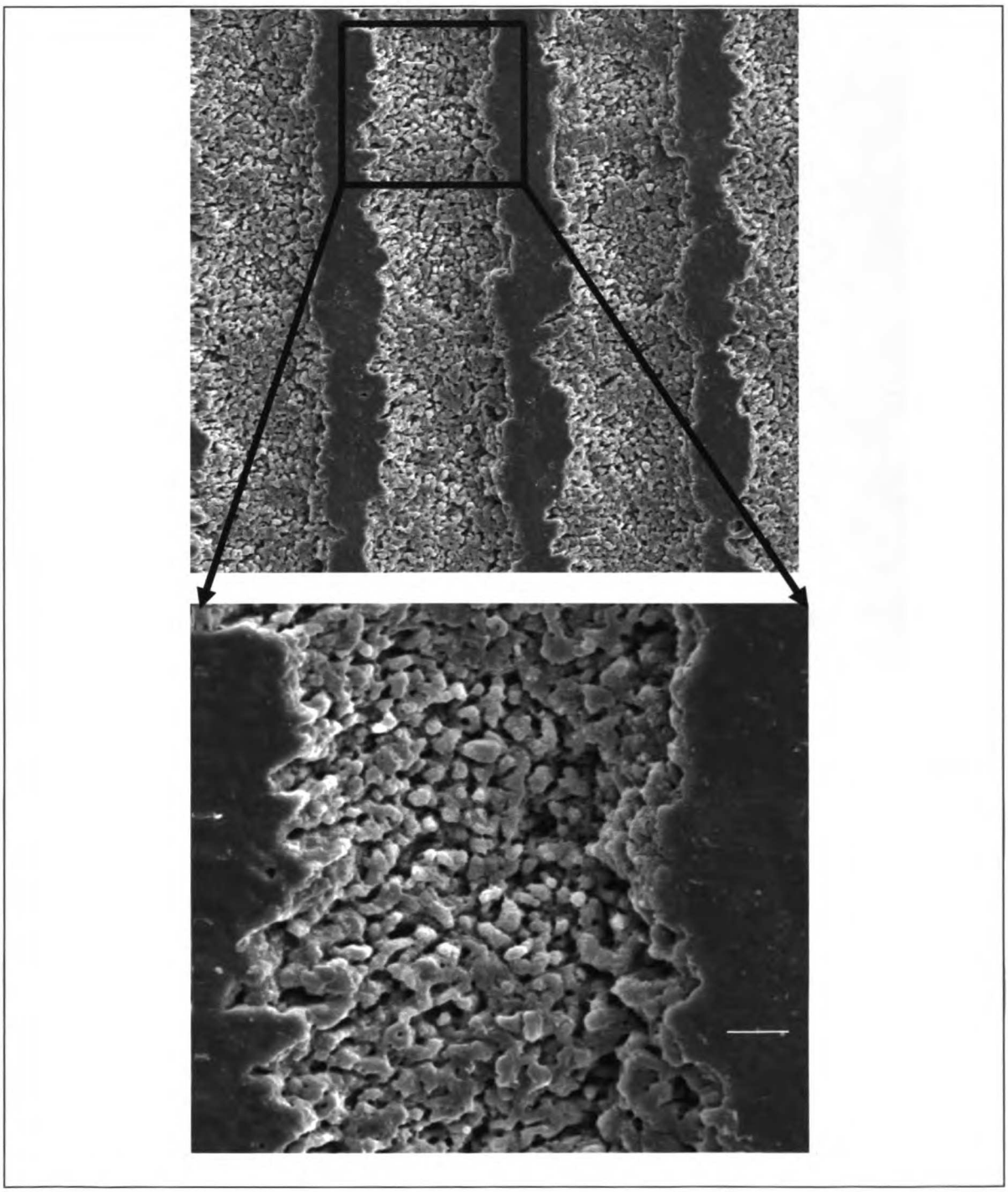

Figure 20. **SEM micrographs (300x and 1000x magnification) of a laser-irradiated sample (fluence 4.2 J/cm^2) clearly show the presence of intact enamel rods (of 4- to 5-µm width) with the inter-prismatic tissue selectively removed. A box depicts the magnified region from the 300x image. Bar= 20 µm.**

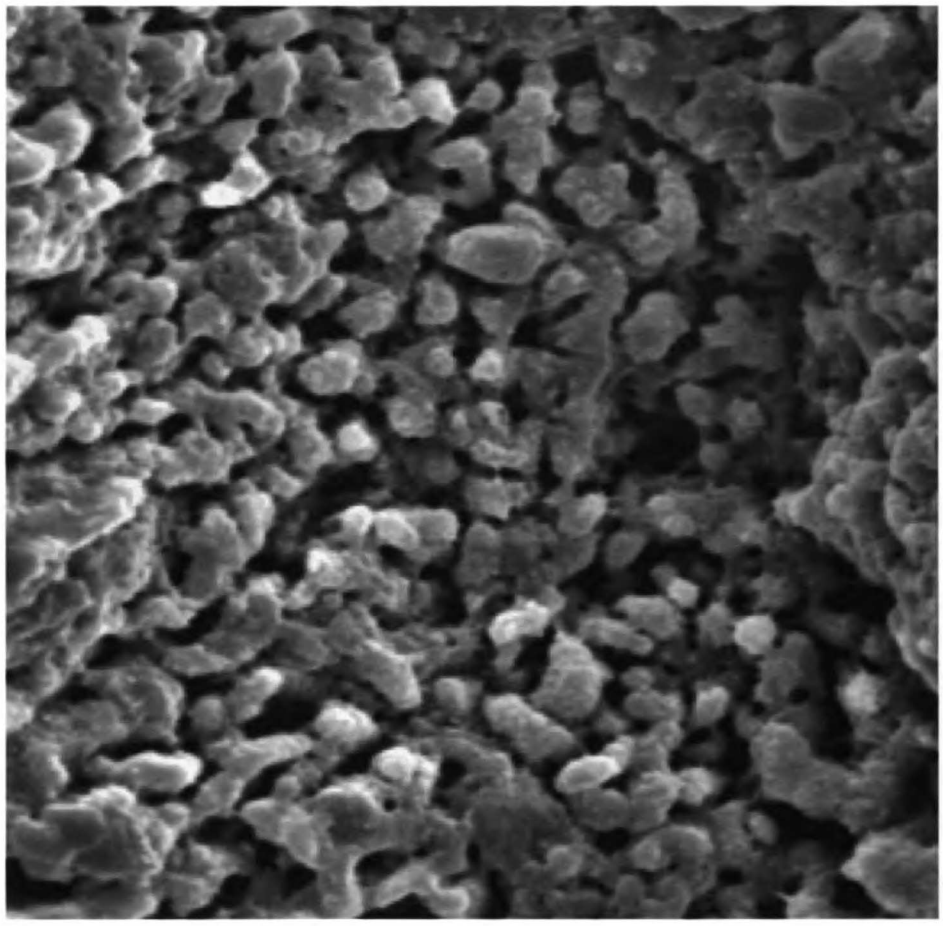

Figure 21. A closer view of the modified surface treated by the Nd:YAG laser at 355 nm (fluence 4.2 J/cm^2).

These micrographs demonstrate that inter-prismatic enamel, having a larger organic component than the prisms or enamel rods themselves, can be selectively ablated resulting in a modified topography suitable for resin bonding. The enamel rods are approximately 4-5 micrometers wide.

Conventional acid etching produces a different pattern of modification, with selective dissolution and removal of the higher mineral-containing prisms. Figure 22, below, demonstrates the type of etching that has been referred to as a Type 1 etch pattern (2000x magnification). [14]

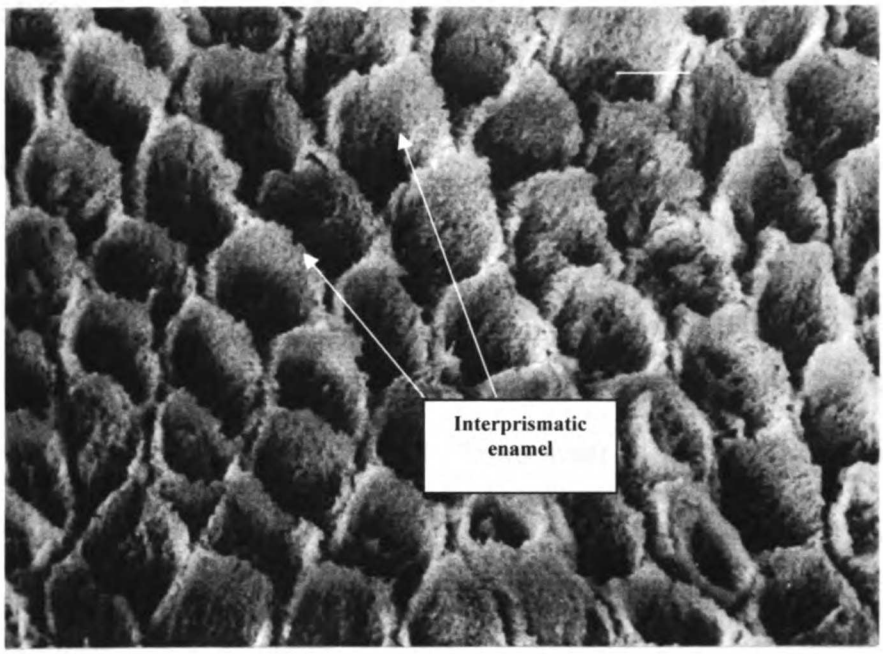

Figure 22. **SEM micrograph (2000x magnification) showing Type I acid etch pattern achieved with 37% ortho-phosphoric acid (15 sec). Bar= 5-µm.**

VI. DISCUSSION

A. Surface Modification and Caries Resistance

These findings demonstrate that near UV laser pulses (λ=355 nm) of 5 nanoseconds duration can be used to modify the surface morphology of bovine enamel. It has been demonstrated that 355-nm laser pulses preferentially ablate the higher organic-containing (protein and lipids) inter-prismatic enamel, leaving the mineral rods themselves relatively intact. Furthermore, these findings demonstrate that such a modification permits an enhanced delivery of fluoride. The laser treatment followed by a one time topical application of fluoride increased the resistance to acid dissolution by nearly 55% over controls.

There have been many reports where laser irradiation alone has produced increases in acid resistance. The CO_2 laser has been widely used to study this phenomenon. The use of CO_2 laser irradiation to achieve enamel crystal fusion and to produce a physiochemical alteration in the enamel for the prevention of caries has been widely demonstrated. [54, 55] Hydroxyapatite, ($Ca_{10}[PO_4]_6[OH]_2$), has its main absorption peak at a wavelength of 9.6μm. When irradiated with the CO_2 laser, the energy is readily absorbed within the mineral. A surface temperature rise to only 400 ° C results in a 30% loss of carbonate. A surface temperature rise to approximately 800 ° C causes the complete loss of carbonate (lost as CO_2 and H_20) from the mineral, thus converting the mineral from

carbonated-apatite to the more acid resistant hydroxyapatite. [8, 9] A temperature rise greater than 1,200 ° C causes momentary melting and fusion of hydroxy-apatite. [7] An increase in resistance to acid challenge and inhibition of caries progression is correlated to the decomposition of carbonate in irradiated enamel mineral. Conversion of carbonated apatite to a hydroxyapatite-like mineral with fewer lattice defects and facilitation of grain growth are the most important structural change to decrease the solubility of enamel. [8, 9]

Featherstone *et al.* have demonstrated a reduction in acid reactivity in enamel, by using a tunable CO_2 laser (at λ=9.3, 9.6, 10.3, and 10.6-μm) covering a wide range of fluences (1 to 12.5 J/cm^2). Inhibition in caries progression was observed, ranging on the order of 40 to 85%, depending on the specific laser conditions applied. [56] The 9.3- and 9.6-μm wavelength settings were very effective, even when low fluences were used, in reducing acid reactivity of treated enamel, meanwhile minimizing subsurface temperature elevations. [56]

Kantorowitz *et al.* reported that by pulsing the CO_2 laser, significant and high increases in caries inhibition were produced. [57] While a single pulse achieved some inhibition, increasing the number of pulses per spot to 25, maximized the degree of inhibition to 87%. If greater than 25 pulses per spot were used, no additional increase in resistance was noted. [57]

The use of near-UV excimer lasers (notably the ArF laser at 193 nm and the KrF laser at 248 nm) has been shown to preferentially and selectively ablate organic phases of both dentin and enamel, thus providing a suitable substrate for dentin and enamel bonding. [11, 58-60] A photochemical model of ablation has

been suggested in which absorption of high energy UV photons by organic tissue elements leads to direct dissociation of the covalent bonds within those tissue elements. [59, 61] In an elevated energy state, the bonding energy is exceeded and atoms are free to dissociate thus resulting in a breaking up of material structure. Very low fluences (1 J/cm^2) can be used to see this effect. [11]

When non-linear optics for 2nd (532 nm), 3rd (355 nm) and 4th (266 nm) harmonics are added to a Q-switch Nd:YAG laser (1064 nm), it can become effective in specifically targeting organic components of enamel. The results in the present study show that the Nd:YAG laser operating in its third harmonic (λ = 355 nm) did not, *as the sole intervention*, result in a decrease in the dissolution rate of acid challenged enamel. In fact, there was a trend for a slight but non-statistically different increase in solubility.

To study the role of lipids in the progression of carious lesions (present in enamel: 0.5% by weight, 1.5% by volume), Featherstone and Rosenberg experimentally removed the lipid prior to acid challenge. They showed that removal of lipids from enamel tissue enhanced caries progression. [62] The slight increase in solubility of enamel (seen in the laser-only group) is likely attributed to the removal of the protective lipid and protein by Nd:YAG ablation. The Nd:YAG laser at 355 nm is able to expose the enamel crystal surfaces to either demineralization, remineralization, or a fluoride treatment environment.

The SEM photomicrographs obtained for this study show that even with low fluences, the subsurface enamel is exposed and the surface appearance is clean and clear of debris. This laser may in fact cause a slight improvement in

acid resistance of irradiated enamel mineral, however due to the large increase in surface area and amount of exposed mineral that comes in contact with the dissolution solution, the increased amount of released calcium and phosphate may mask the beneficial effects of laser treatment to the mineral microstructure.

Laser irradiation prior to fluoride application causes a synergistic effect in vastly lowering acid solubility of the combined treated enamel. The finding in this study showed nearly a 54% inhibition in acid dissolution using a one-time APF (1.23% F) fluoride treatment. Huang *et al.* (2001) also reported a synergistic effect by utilizing Nd:YAG laser irradiation (continuous wave; λ=1064 nm) prior to the application of a high-content fluoride varnish (Colgate-Palmolive Duraphat; 5%NaF; Canton, MA) showing nearly an 80% reduction in artificial caries on smooth surfaces. [63] To achieve these high reductions in acid reactivity, prohibitively high fluences were used (2.5 Watts, 6 seconds).

The underlying mechanisms causing a *synergistic* effect on caries inhibition via laser treatment and topical application of fluoride are not completely understood. It is likely that the frequency-tripled Nd:YAG laser, like the excimer lasers, are able to selectively ablate the inter-prismatic enamel, due to the presence of protein, and expose the enamel prisms to leave a relatively homogenous, mineral-rich tissue. Such a mineral, rich in carbonated hydroxyapatite, is amenable to surface conversion to fluorapatite, in the presence of fluoride, calcium, and phosphate.[38]

Tagomori reported that APF application *after* Nd:YAG laser irradiation produces a greater fluoride uptake in enamel than APF application *before* laser

treatment. [64] When fluoride was applied before laser irradiation, the synergistic effect was lost. Nd:YAG laser (λ = 355 nm) irradiation creates a roughened surface morphology through ablation of lipid and protein in the prism boundaries thus providing a path for penetration of fluoride ion deep into these crevasses and influencing fluoride uptake. [65-67] Then conversion of carbonated apatite to fluorapatite [38] may occur at relatively deep levels, depending upon the depth of protein and lipid ablation and infiltration of fluoride.

Due to the minute amount of organics within the enamel structure, it is impossible for the FTIR spectrophotometer to detect a change in the protein and lipid content in enamel. Studies on dentin have demonstrated this effect however. The fact that the carbonate peak remains present in the FTIR, in spite of near-UV laser irradiation (at 355 nm), supports the notion of selective protein targeting. A non-selective ablative process would likely induce a sufficient thermal effect to drive carbonate from the mineral.

B. Laser Modification and Bonding

These findings demonstrate that using near UV laser pulses (λ = 355 nm) of 5 nanoseconds duration, the bovine enamel surface morphology can be sufficiently modified to permit a clinically significant bonding of an orthodontic attachment, using commercially available resin adhesive agents. Many researchers have failed to obtain bond strengths comparable to the results presented in this paper. This discrepancy lies partly within the laser systems and

wavelengths used, and partly with waveform used. Continuous and long-pulsed laser systems would induce an excessive thermal effect that would result in a smooth, glass-like ("vitrified") enamel surface. Although a smooth surface would be suitable for caries resistance, it provides little retention for restorative and adhesive resins.

Ariyaratnam *et al.* used a pulsed Nd:YAG laser system operating at 1064-nm and found disappointing shear bond test results ranging from 4.6 to 8.8 MPa.[32] Since there is little surface absorption of the Nd:YAG laser beam when operating at 1064 nm, little surface modification would be expected regardless of fluence used. Von Fraunhofer attempted to address this problem with the Nd:YAG laser at 1064-nm by placing a light-absorbing black ink on the buccal surfaces of the subjects' teeth prior to laser etching to receive direct bonding of orthodontic attachments. In addition to requiring a clinically laborious step to add such a dye, the results were disappointing as a high number of clinical failures were observed.[66]

The Er:YAG laser has been well reported to be very efficient in hard tissue ablation.[67-69] The 2.94-μm wavelength closely approximates the absoption of water. Both enamel and dentin can be removed in part by a continuous vaporization process and, in part, in the form of micro-explosions. Continuous vaporization occurs in the range of high fluences (explained by the linear relationship between crater depth and radiant exposure). Micro-explosions are the result of a high-pressure buildup within the mineral due to rapidly heated water, resulting in loss of tissue. Since there is only the small water content

(higher in dentin than enamel) needs to be vaporized, lower fluences are necessary for this ablation process (explained by a logarithmic relation between crater depth and radiant exposure). [67] Even lower fluences could be used when an exogenous cooling stream of water is applied to the irradiated surface, thus achieving a high degree of safety, as viewed from a thermal standpoint. [68, 69]

The results in this study clearly show that superior bond strengths are achieved when using the gold standard of conventional acid etching. However while being statistically different from controls, clinically significant bond strengths can be achieved with the use of laser-irradiated etching. It has been reported that shear bond strengths of approximately 6 MPa has been suggested to be the minimum clinically acceptable bond strength for direct bonded orthodontic attachments. [66, 70, 71] The bond strengths observed in this study, for each of the fluences tested, are vastly greater than the reported minimum acceptable level yet are not too high that would make bracket removal difficult at the time of debond.

The bond strengths reported in this study are slightly higher than those reported with resin-reinforced glass ionomer adhesives. [31] Resin-reinforced glass ionomers have become clinically accepted, and widely used alternatives to acid etching/resin bonding of orthodontic attachments. Their inherent ability to bond chemically to the mineral surface, release and re-release fluoride, and reduce demineralization along the periphery of brackets and attachments have stimulated such an interest, notwithstanding their lower bond strengths.

Acid etching does have some disadvantages. Among these is the uncontrollable depth of etching (up to 100 micrometers in depth). Second, the pattern of etching type is unpredictable. Etch time and enamel rod orientation affect etch pattern. [72, 73] Thirdly, acid residues can be isolated even after thorough irrigation (transiently up to 40% of the original acid concentration). The likelihood of long-term sequellae to this residual acid is probable, although it would be very difficult to quantify its effect. Finally, the geometry and the extent of the etched area are impossible to reproduce clinically. [35] While white spot lesions are commonly observed in orthodontic patients, it seems counterintuitive to purposely use an acid etchant during appliance placement, while throughout the remainder of the treatment, prescribe strict oral hygiene to reduce the accumulation of acid byproducts from oral microbes.

C. Summary and Future Directions for Research

A novel method for increasing bond strengths of restorative materials and enhancing fluoride delivery with the goal of increasing caries inhibition with the use of a frequency-tripled Nd:YAG laser (λ=355 nm) was demonstrated in this study. The advantages of using this protocol are clear. The modification of the enamel surface due to laser irradiation is a clean process enabling the bonding of orthodontic attachments, with moderately high, clinically acceptable bond strengths. Simultaneously, the modification exposes the enamel mineral, enabling a fluoride application to render the surface enamel prisms much more resistant to acid challenge. Such a protocol obviates the need for resin-

reinforced glass ionomer cements, which many orthodontic practitioners have relied upon to reduce the incidence of white spot lesions.

Previous researchers, using the same Nd:YAG laser (and laser conditions) utilized in this study, have demonstrated that laser irradiation with λ = 355 nm can remove, with a high degree of selectivity, residual composite that is left on the surfaces of teeth after de-bonding of orthodontic attachments. [49] Furthermore, considering the low fluences used and the selective targeting of organics and polymers, it was observed that only a negligible increase in pulpal temperature occurs as measured by thermocouple experiments. [49] Combining this margin of safety with the demonstration that this laser can perform a wide variety of tasks, the reality of having a widely accepted, everyday laser system in every dental office is attainable.

Further studies following the work in this study should focus on the effect of fluoride on bond strength. Furthermore, it should be investigated if different preparations and concentrations of topical fluoride (acidulated phosphate fluoride, sodium fluoride, stannous fluoride, or monofluorophospahate) or vehicle of delivery (gels, foams, or varnishes) further enhance the delivery of fluoride. In other words, the optimal formulation should be investigated where deep penetration of fluoride ion into the depths of the pores and valleys of the exposed, irradiated enamel crystal surfaces is ensured. The fact that this laser system effectively enhances fluoride delivery and achieves suitable bond strengths to enamel merits a similar application and investigation with dentin. In

addition, bond strength studies should be investigated with a wide spectrum of commercially available restorative resins.

It is prudent that these findings be applied in an *in vivo* setting to validate the claims made in the laboratory. This, coupled with the discovery of new, faster, and more efficient laser systems, and the identification of optimal laser operating conditions, will continue to move the field in a healthy direction.

VII. REFERENCES

1. Liberman R, Segal TH, Nordenberg D, Serebro LI. Adhesion of compsite materials to enamel: comparison between the use of acid and lasing as pretreatment. *Lasers Surg Med.* 1984;4:323-327.

2. Cooper LF, Myers ML, Nelson DGA, Mowery AS. Shear strength of composite bonded to laser-pretreated dentin. *J Prosth Dent.* 1988;60:45-49.

3. Dederich DN, Hinkelman KW, Albert A, Tulip J. Effect of CO_2 laser on dentinal bonding. *SPIE Proc.* 1990;1200:420-424.

4. Dederich DN, Tulip J. The effect of Nd:YAG laser on dentinal bond strength. *SPIE Proc.* 1991;1424:134-137.

5. Fried D, Glena RE, Featherstone JDB, Seka W, The nature of light scattering in dental enamel and dentin at visible and near infrared wavelengths. *Applied Optics.* 1995;34:1278-1285.

6. Fried D, Glena RE, Featherstone JD, Seka W. Permanent and transient changes in the reflectance of CO_2 laser-irradaited dental hard tissues at

lambda= 9.3, 9.6, 10.3, and 10.6 microns and at fluences of 1-20 J/cm^2. *Lasers Surg Med.* 1997; 20:22-31.

7. Wigdor HA, Walsh JT, Featherstone JD, Visuri SR, Fried D, Waldvogel JL. Lasers in dentistry. *Lasers Surg Med.* 1995;16:103-133.

8. Zuerlein MJ, Fried D, Featherstone JDB. Depth profile of the chemical and morphological changes of CO_2 laser irradiated dental enamel. *SPIE.* 1999;3593:204-209.

9. Zuerlein MJ, Fried D, Featherstone JDB. Modeling the modification depth of carbon dioxide laser-treated dental enamel. *Lasers Surg Med.* 1999;25:335-347.

10. Spitzer D, Bosch JT. The absorption and scattering of light in bovine and human dental enamel. Calcif Yissue Res. 1975:17:129-137.

11. Moss JP, Patel BCM, Pearson GJ, Arthur G, and Lawes RA. Krypton fluoride excimer laser ablation of tooth tissues: precision tissue matching. *Biomaterials.* 1994;13:1013-1018.

12. Hess JA. Subsurface morphologic changes of Nd:YAG laser-etched enamel. *Lasers Surg Med* 1997;21:193-197.

13. Buonocore MG. A simple method of increasing the adhesion of acrylic filling materials to enamel surfaces. *J Dent Res.* 1955;34:849-853.

14. Silverstone LM, Saxton CA, Dogon IL, Fejerskov O: Variation in the pattern of acid etching of human dental enamel examined by scanning electron microscopy. *Caries Res.* 1975;9:373-387.

15. Costa LRRS, Watanabe I, Fava M. Three-dimensional aspects of etched enamel in non-erupted deciduous teeth. *Braz Dent J.* 1998;9:95-100.

16. Zidam O, Hill G. Phosphoric acid concentration: enamel loss and bonding strength. *J Prosthet Dent.* 1986;55:388-392.

17. de Goes MF, Sinhoreti MAC, Consani S, da Silva MAP. Morphological effect of the type, concentration and etching time of acid solutions on enamel and dentin surfaces. *Braz Dent J.* 1998;9:3-10.

18. Gwinnett AJ, Garcia-Godoy F. Effect of etching time and acid concentration on resin shear bond strength to primary tooth enamel. *Am J Dent.* 1992;5:237-239.

19. Gwinnett AJ, Ceen RF. Plaque distribution on bonded brackets: a scanning microscope study. *Am J Orthod.* 1979;75:667-677.

20. Saloum FS, Sondhi A. Preventing enamel decalcification after orthodontic treatment. *JADA.* 1987;115:257-261.

21. Featherstone JDB, Glena R, Shariati M, Shields CP. Dependence of *in vitro* demineralization and re-mineralization of dental enamel on fluoride concentration. *J Dent Res.* 1990;69:620-625.

22. Zachrisson BJ. A post-treatment evaluation of direct bonding in orthodontics. *Am J Orthod.* 1977;71:173-89.

23. Gorelick L, Geiger AM, Gwinnett AJ. Incidence of white spot formation after bonding and banding. *Am J Orthod.* 1982;81:93-98.

24. Ogaard B. Prevalence of white spot lesions in 19-year-olds: a study on untreated and orthodontically-treated persons 5 years after treatment. *Am J Orthod Dentofacial Orthop.* 1989;96:423-427.

25. Hargreaves JA, Thompson GW, Wagg BJ. Changes in caries prevalence in Isle of Lewis children between 1971 and 1981. *Caries Res.* 1983;17:554-559.

26. Jenkins GN. Recent changes in dental caries. *Br Med J.* 1985;291:1297-1298.

27. Van Louveren C. The anti-microbial action of fluoride and its role in caries inhibition. *J Dent Res.* 1990;69:620-625.

28. Featherstone JDB. The science and practice of caries prevention. *JADA.* 2000;131:887-899.

29. Nelson DG, Featherstone JD, Duncan JF, Cutress TW. Effect of carbonate and fluoride on the dissolution behavior of synthetic apatities. *Caries Res.* 1983;17:200-211.

30. Moreno EC, Kresak M, Zahradnick RT. Physiochemical aspects of fluoride-apatite systems relevant to the study of dental caries. *Caries Res.* 1977;11:142-171.

31. Kantorowitz, Z. The feasibility of bonding orthodontic brackets to laser treated enamel surfaces. Master's Thesis. 1998.

32. Ariyaratnam MT, Wilson MA, Mackie IC, Blinkhorn AS. A comparison of surface roughness and composite/enamel bond strength of human enamel

following the application of the Nd:YAG laser and etching with phosphoric acid. *Dent Mater.* 1997;13:51-55.

33. Fuhrmann R, Gutknecht N, Magunski A, Lampert F, Diedrich P. Conditioning of enamel with Nd:YAG and CO_2 dental laser systems and with phosphoric acid: an in-vitro comparison of the tensile bond strength and the morphology of the enamel surface. J Orofac Orthop. 2001;62:375-386.

34. Martinez-Insua A, Da Silva Dominguez L, Rivera FG, Santana-Penin UA. Differences in bonding to acid-etched or Er:YAG-laser-treated enamel and dentin surfaces. J Prosthet Dent. 2000;84:280-288.

35. Stratmann U, Schaarschmidt K, Schürenberg M, Ehmer U. The effect of ArF-excimer laser irradiation of the human enamel surface on the bond strength of orthodontic appliances. *Scanning Microscopy.* 1995;9:469-478.

36. Hsu J, Fox JL, Wang Z, Powell GL, Otsuka M, Higuchi WI. Combined effects of laser irradiation/solution fluoride ion on enamel demineralization. J Clin Laser Med Surg. 1998;16:93-105.

37. Fox JL, Yu D, Otsuka M, Higuchi WI, Wong J, Powell GL. Initial dissolution rate studies on dental enamel after CO_2 laser irradiation. *J Dent Res.* 1992;71:1389-1398.

38. Phan ND, Fried D, Featherstone JDB. Laser-induced transformation of carbonated apatite to fluorapatite on bovine enamel. *Lasers In Dentistry V SPIE.* 1999;3593:233-240.

39. Tagomori S, Morioka T. Combined effects of laser and fluoride on acid resistance of human dental enamel. *Caries Res.* 1989;23:225-231.

40. Fox NA, McCabe JF, Buckley JG. A critique of bond strength testing in orthodontics. *Br J Orthod.* 1994;21:33-43.

41. Katona TR. The effects of load location and misalignment on shear/peel testing of direct bonded orthodontic brackets--a finite element model. *Am J Orthod Dentofacial Orthop.* 1994;106:395-402.

42. Bishara SE, Olsen M, Von Wald L. Comparison of shear bond strengths of precoated and uncoated brackets. *Am J Orthod Dentofacial Orthop.* 1997;112:617-621.

43. Watanabe LG, Lacy AM, Davis DR. Shear bond strength: single plane versus conventional lap shear. *J Dent Res.* 1987;67:383, Abst 2159.

44. Watanabe LG, Marshall WG, Marshall SJ. Dentin shear strength: effects of tubule orientation and intra-tooth location. *Dent Mater.* 1996;12:109-115.

45. White JM, Goodis HE, Marshall SJ, Marshall GW. Sterilization of teeth by gamma radiation. *J Dent Res.* 1994;73:1560-1567.

46. Smith HZ, Casko JS, Leinfelder KF, Utleu JD. Comparison of orthodontic bracket bond strengths: human versus bovine enamel. *J Dent Res.* 1976;55:B153, Abst. 367.

47. Nakamichi I, Iwaku M, Fusayama T. Bovine teeth as possible substitutes in the adhesion test. *J Dent Res.* 1983;62:1076-1081.

48. Silva CM, Cordazzi JL, Pereira JC, Francishone CE. Shear bond strength of an adhesive system in human, bovine, and swinish teeth. *J Dent Res.* 1996;75:393, Abst. 3005.

49. Alexander R, Xie J, Fried D. Selective removal of residual composite from dental enamel surfaces using the third harmonic of a Q-switched Nd:YAG laser. *Lasers Surg Med.* 2002;30:240-245.

50. Sturdevant CM, Roberson TM, Heyman HO, Sturdevant JR (eds.). The Art and Science of Operative Dentistry. St. Louis: Mosby, 1995).

51. Zanata RL, Navarro MF, Ishikiriama A, da Silva e Souza Junior MH, Delazari RC. *Braz Dent J.* 1997;8:73-78.

52. LeGeros RZ. Calcium phosphates in oral biology and medicine. In Myers HM (ed.). Monographs in oral science. Karger, Basel. 1991;15:108-129.

53. Nelson DGA; Featherstone JDB. Preparation, analysis, and characterization of carbonated apatites. Calcif Tissue Int. 1983;34:S69-S81.

54. Walsh LJ, Perham SJ. Enamel fusion using a carbon dioxide laser: a technique for sealing pits and fissures. *Clin Prev Dent.* 1991;13:16-20.

55. Nelson DG, Shariati M, Glena R, Shields CP, Featherstone JDB. Effect of pulsed low energy infrared laser irradiation on artificial caries-like lesion formation. *Caries Res.* 1986;20:289-299.

56. Featherstone JDB, Barrett-Vespone NA, Fried D, Kantorowitz Z, Seka W. CO_2 laser inhibitor of artificial caries-like lesion progression in dental enamel. *J Dent Res.* 1998;77:1379-1403.

57. Kantorowitz Z, Featherstone JD, Fried D. Caries prevention by CO_2 laser treatment: dependency on the number of pulses used. *JADA*. 1998;129:585-591.

58. Neev J, Liah L-HL, Raney DV, Fujishige JT, Ho PD, Berns MW. Selectivity, efficiency, and surface characteristics of hard dental tissues ablated with ArF pulsed excimer lasers. *Lasers Surg Med*. 1991;11:499-510.

59. Feuerstein O, Palanker D, Fuxbrunner A, Lewis A, Deutsch D. Effect of the ArF excimer laser on human enamel. *Lasers Surg Med*. 1992;12:471-477.

60. Arima M, Matsumoto K. Effects of ArF excimer laser irradiation on human enamel and dentin. *Lasers Surg Med*. 1993;13:97-105.

61. Frentzen M, Koort HJ, Thiensiri I. Excimer lasers in dentistry: future possibilities with advanced technology. *Quintessence Int*. 1992;23:117-33.

62. Featherstone JD, Rosenberg H. Lipid effect on the progress of artificial carious lesions in dental enamel. Caries Res. 1984;18:52-55.

63. Huang GF, Lan WH, Guo MK, Chiang CP. Synergistic effect of Nd:YAG laser combined with fluoride varnish on inhibition of caries formation in dental pits and fissures in vitro. *J Formos Med Assoc*. 2001;100:181-185.

64. Tagomori S, Iwase T. Ultrastructural change of enamel exposed to a normal pulsed Nd:YAG laser. *Caries Res.* 1995;29:513-520.

65. Bahar A, Tagomori S. The effect of normal pulsed Nd-YAG laser irradiation on pits and fissures in human teeth. *Caries Res.* 1994;28:460-467.

66. von Fraunhofer JA, Allen DJ, Orbell, GM. Laser etching of enamel for direct bonding. *The Angle Orthod.* 1993;63:73-76.

67. Hibst R, Keller U. Experimental studies of the application of the Er:YAG laser on dental hard substances: measurement of the ablation rate. *Lasers Surg Med.* 1989;9:338-344.

68. Visuri SR, Walsh JT, Wigdor HA. Erbium laser ablation of dental hard tissue: effect of water cooling. *Lasers Surg Med.* 1996;18:294-300.

69. Visuri SR, Gilbert JL, Wright DD, Wigdor HA, Walsh JT. Shear strength of composite bonded to Er:YAG laser-prepared dentin. *Dent Res.* 1996;75:599-605.

70. Reynolds IR, von Fraunhofer JA. Direct bonding of orthodontic brackets: A comparative study of adhesives. *Brit J Orthod.* 1976;3:143-146.

71. Parmeswaran D, Ganesan S, Ratna P, Koteeswaran D. Comparison of bond strength and surface morphology of dental enamel for acid and Nd-YAG laser etching. *SPIE.* 1999;3593:86-90.

72. Oliver RG. The effects of differing etch times on the etch pattern on enamel of unerupted and erupted human teeth examined using the scanning electron microscope. *Br J Orthod.* 1987;14:105-107.

73. Zidam O, Hill G. Phosphoric acid concentration: enamel loss and bonding strength. *J Prosthet Dent.* 1986;55:388-392.

VIII. APPENDIX

Phosphate Dissolution Graphs--Controls

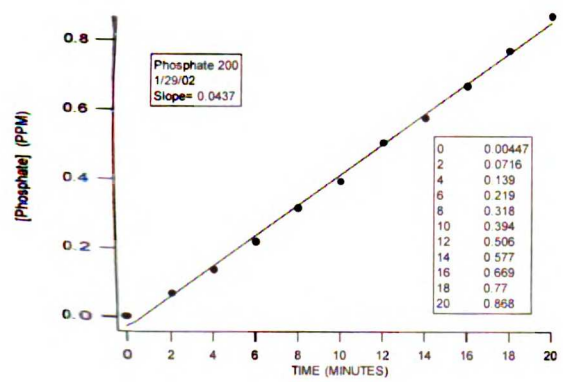

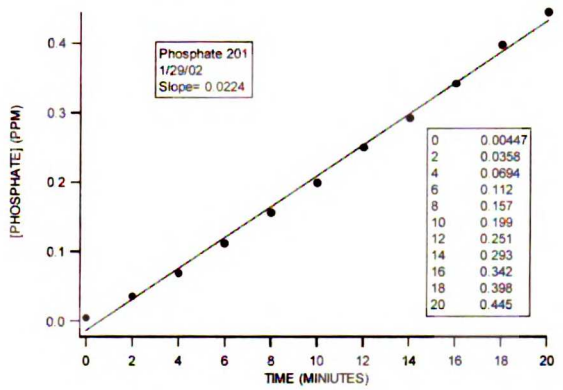

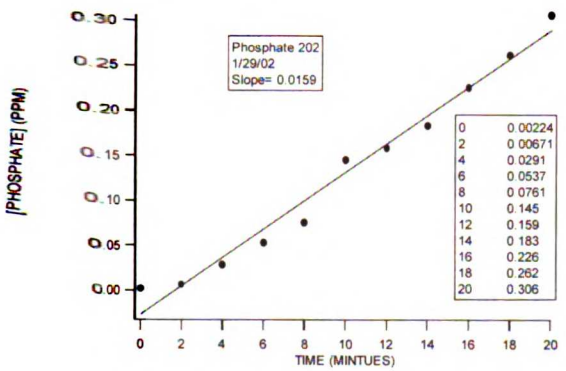

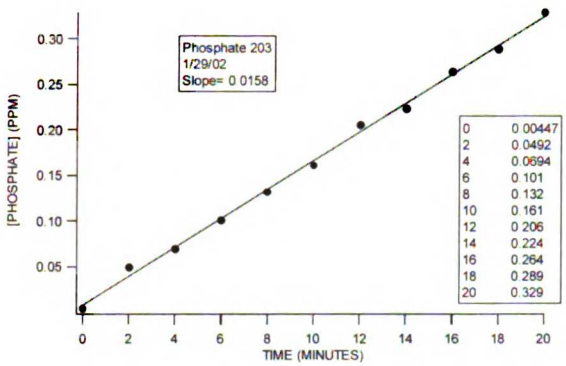

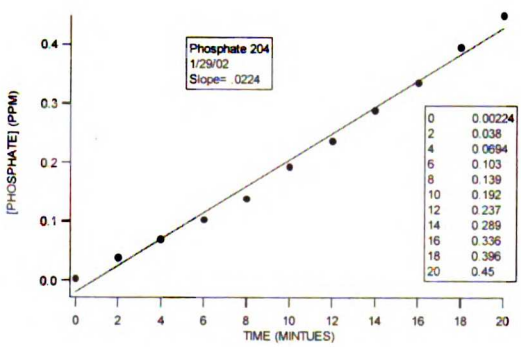

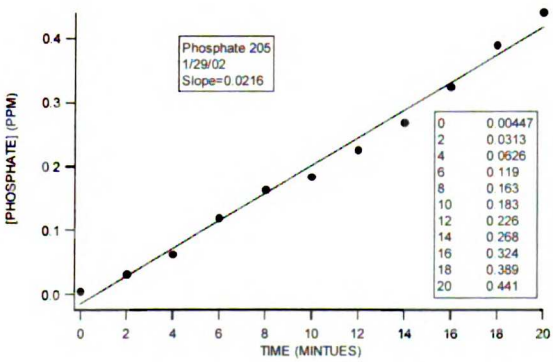

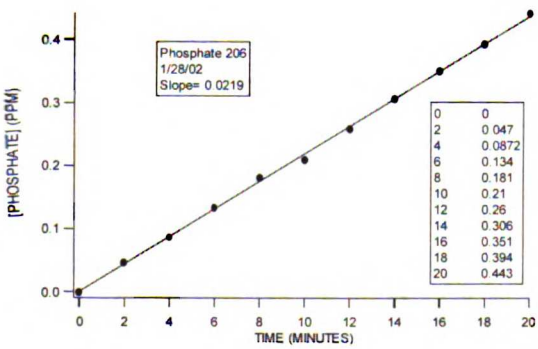

Phosphate Dissolution Graphs—Laser Only

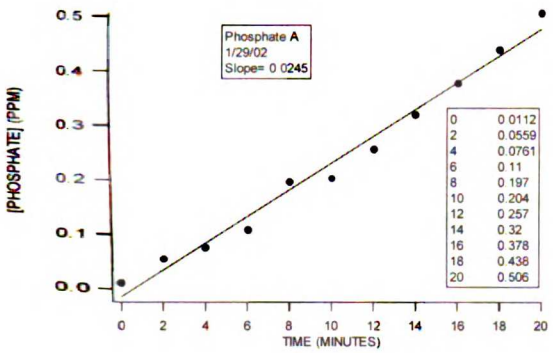

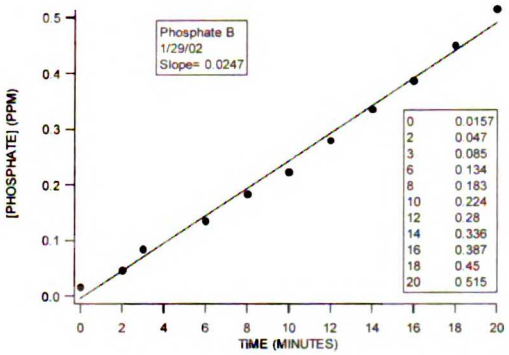

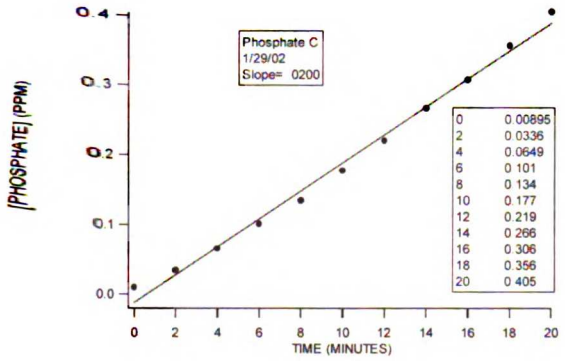

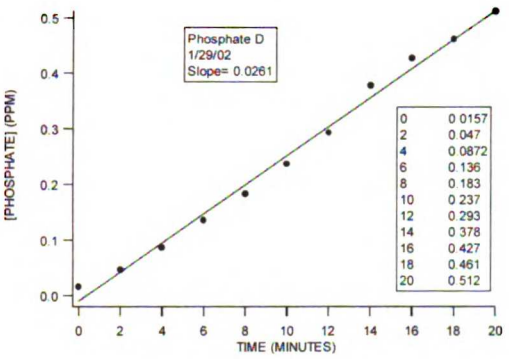

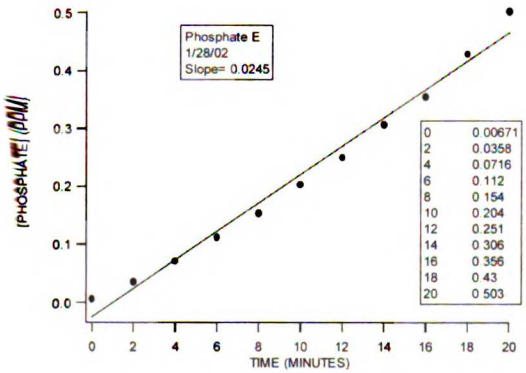

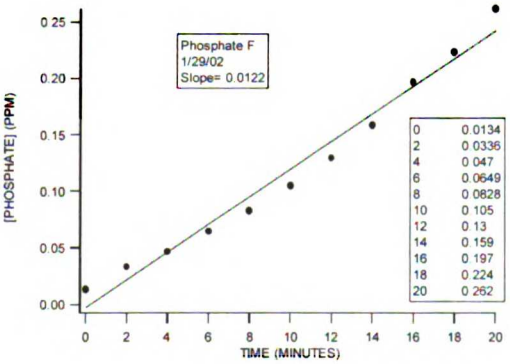

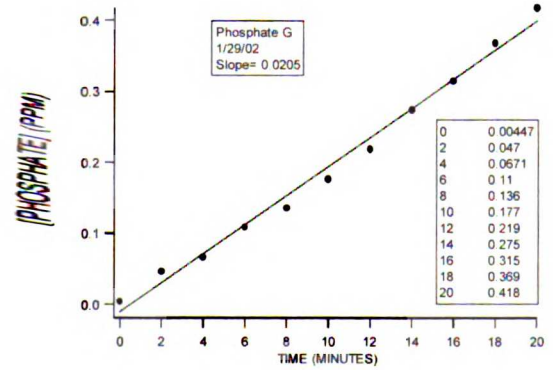

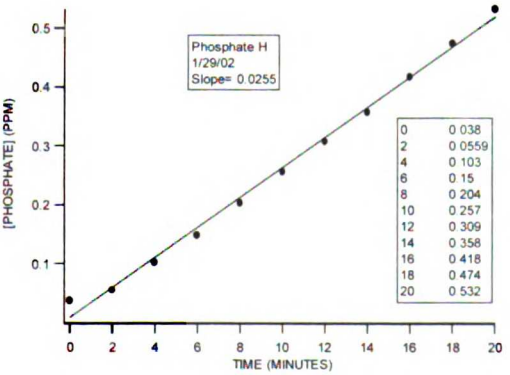

Phosphate Dissolution Graphs—Fluoride Only

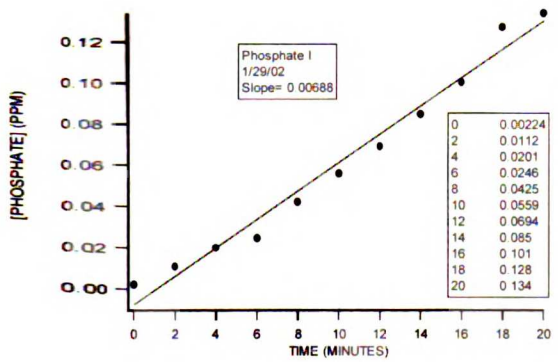

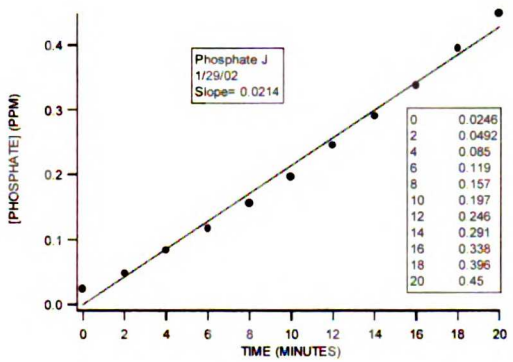

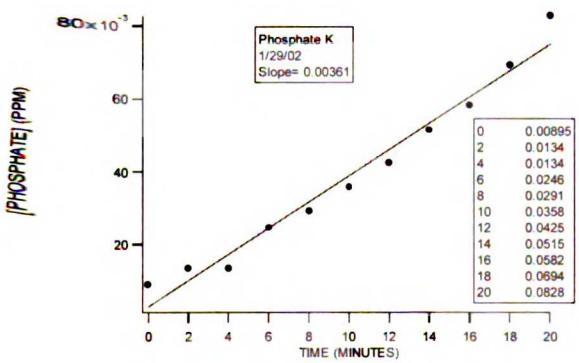

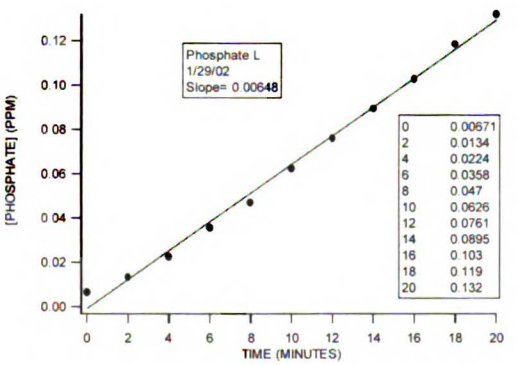

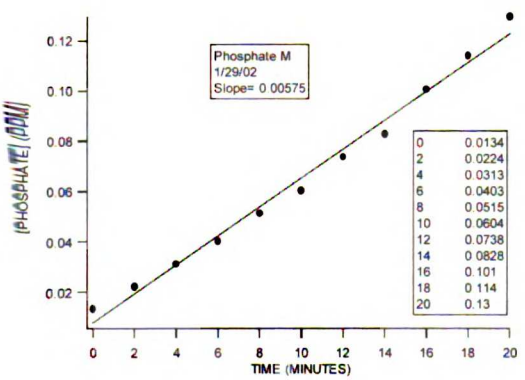

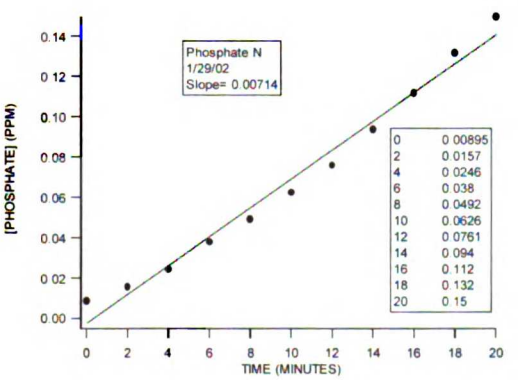

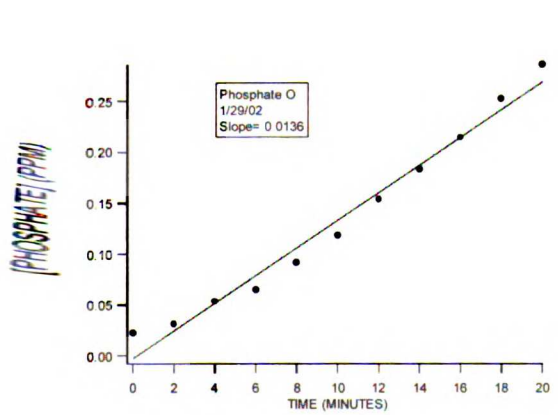

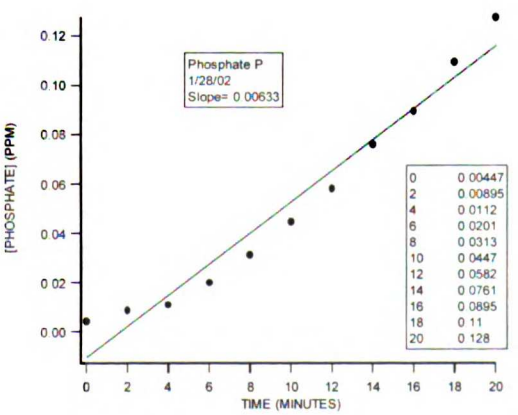

Phosphate Dissolution Graphs—Laser and Fluoride

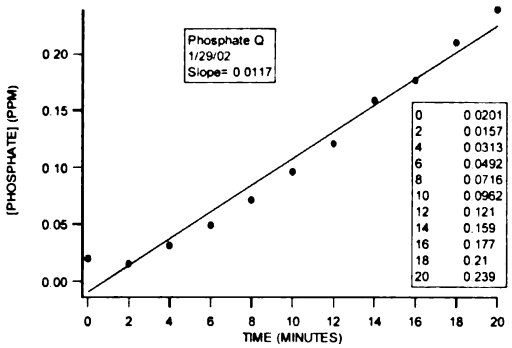

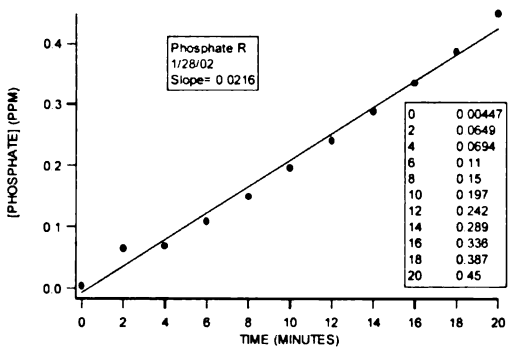

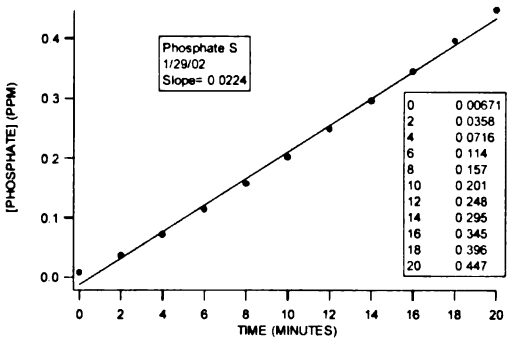

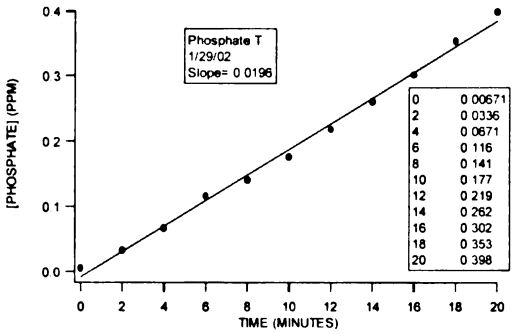

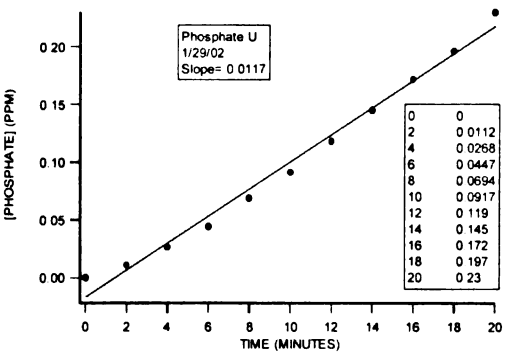

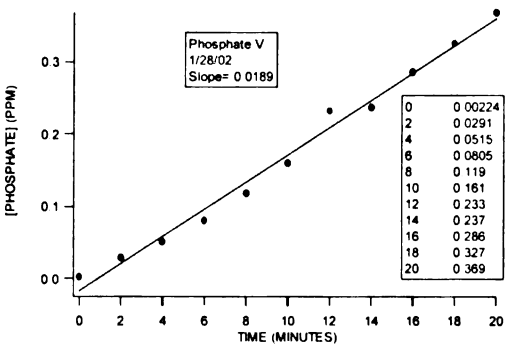

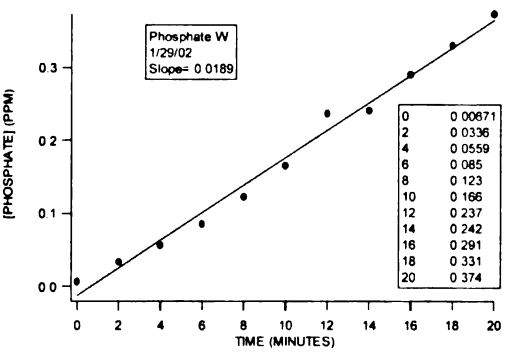

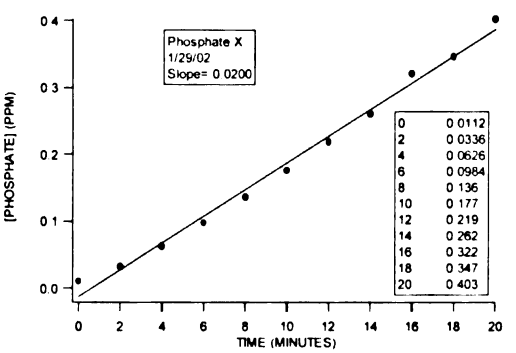

Calcium Dissolution Graphs--Controls

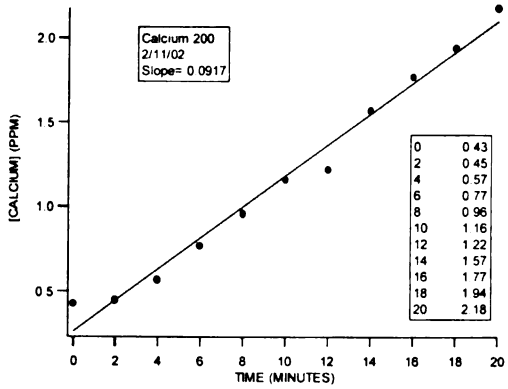

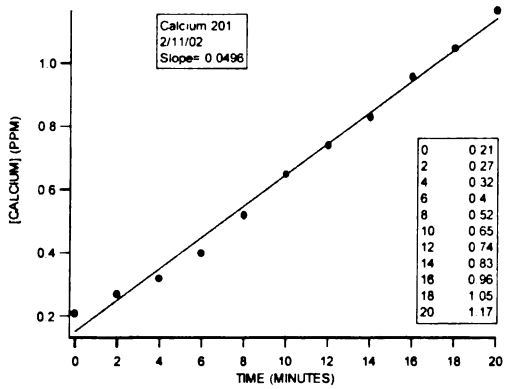

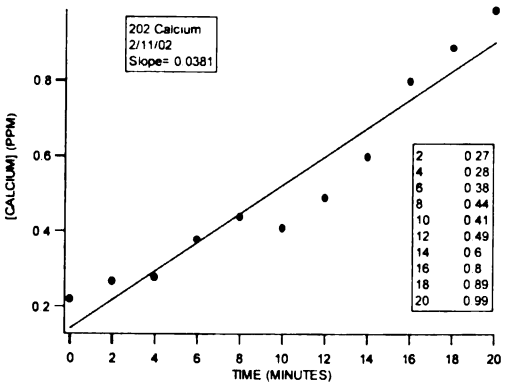

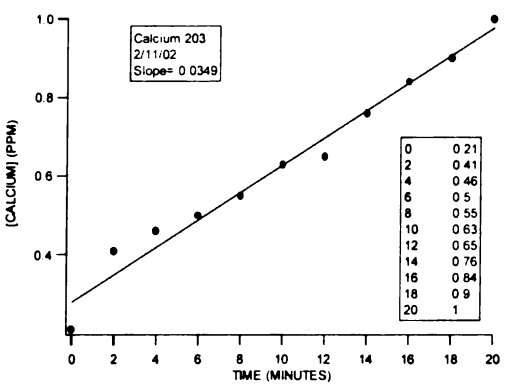

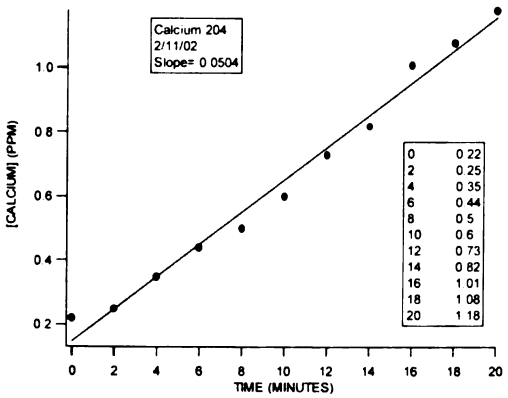

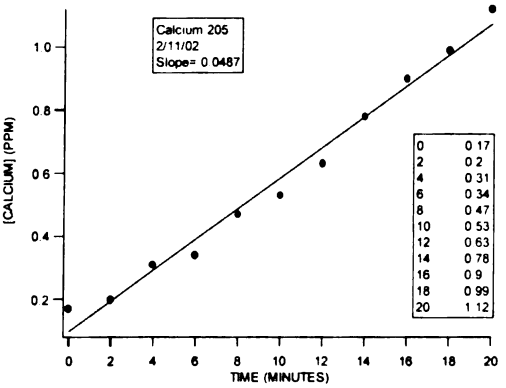

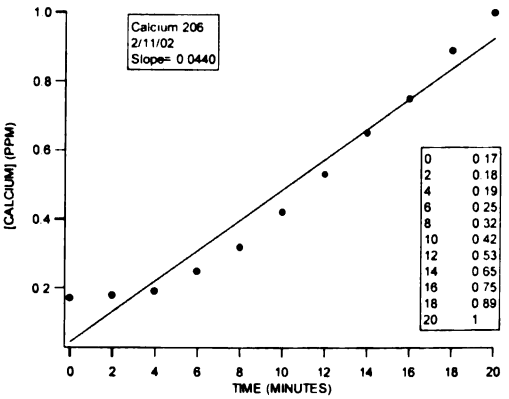

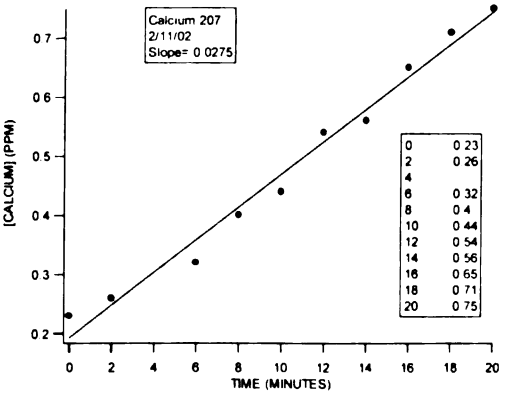

Calcium Dissolution Graphs—Laser Only

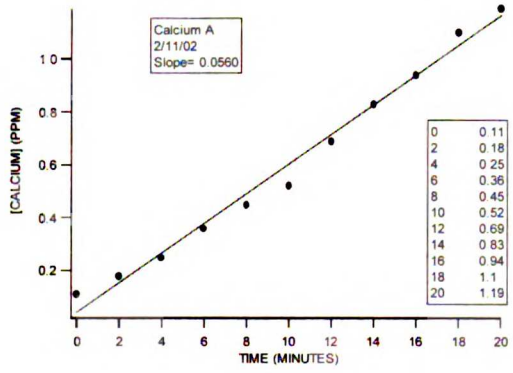

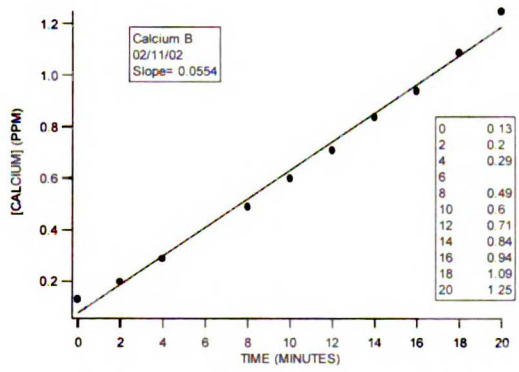

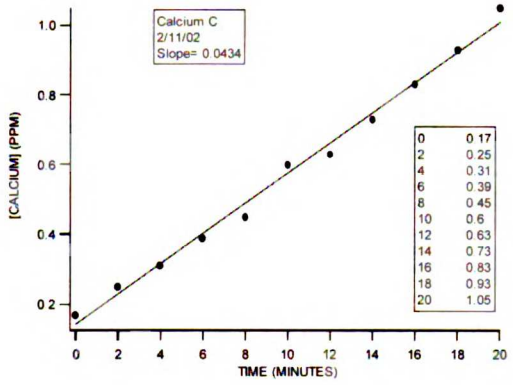

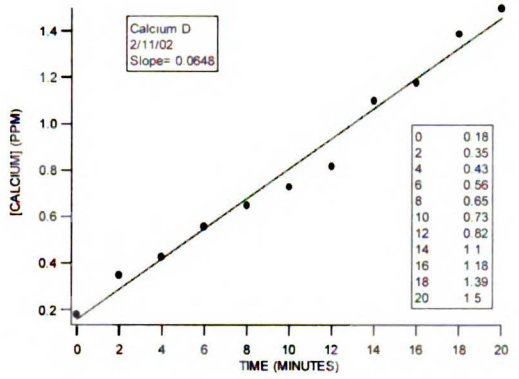

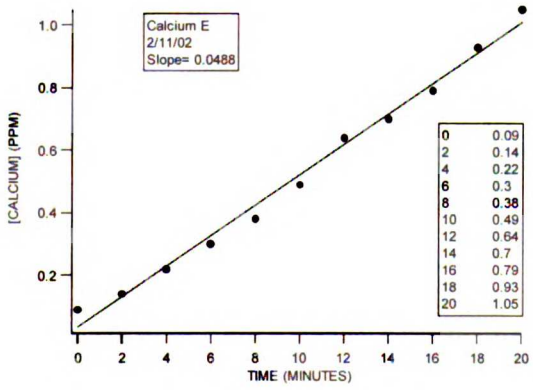

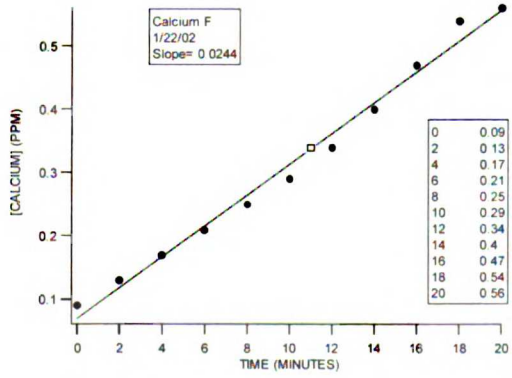

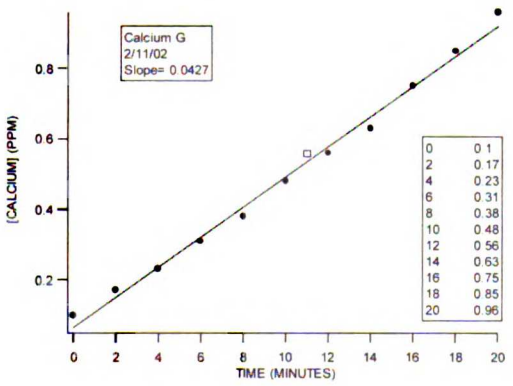

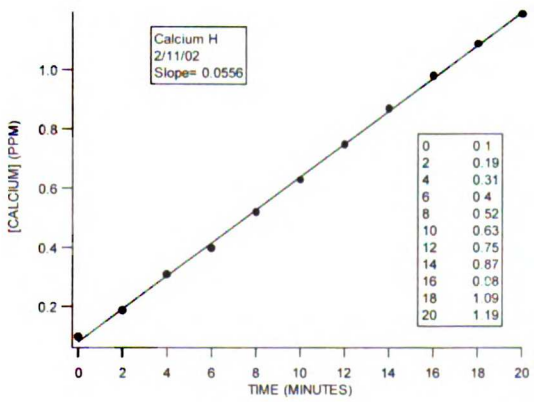

Calcium Dissolution Graphs—Fluoride Only

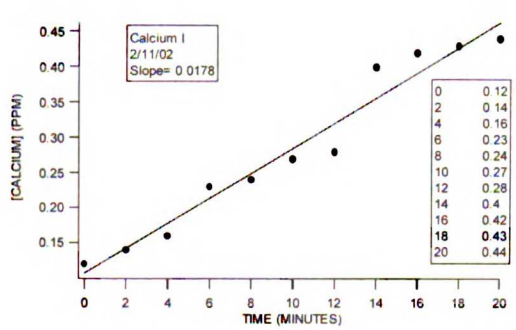

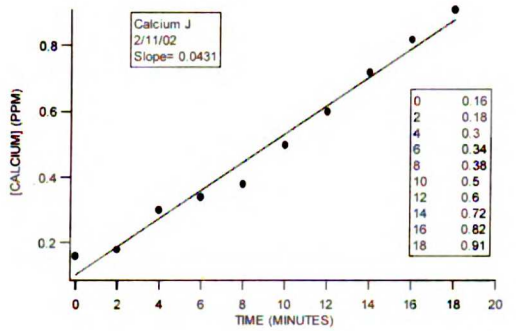

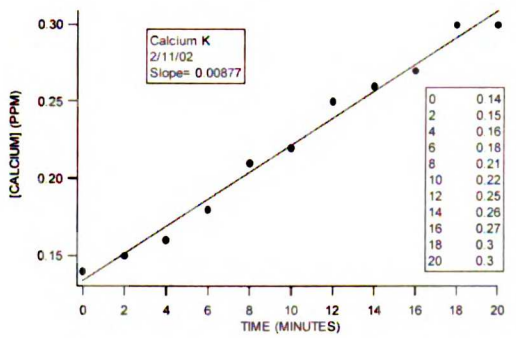

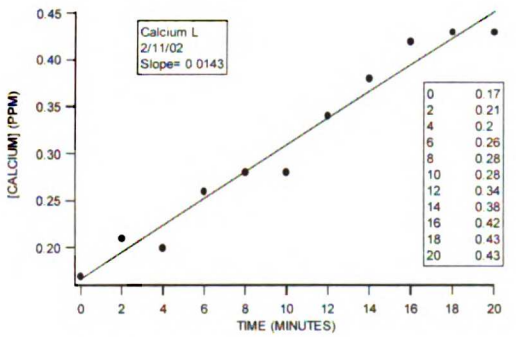

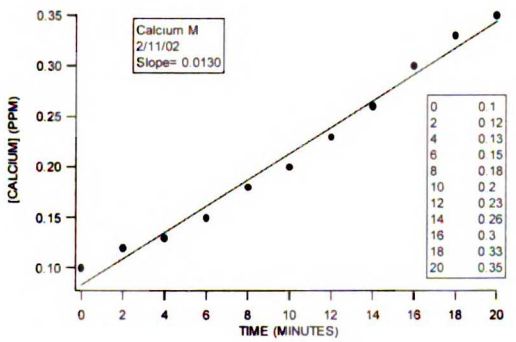

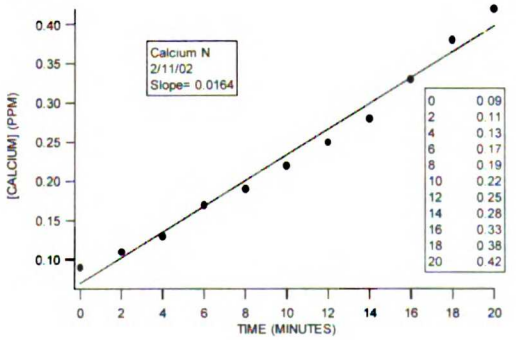

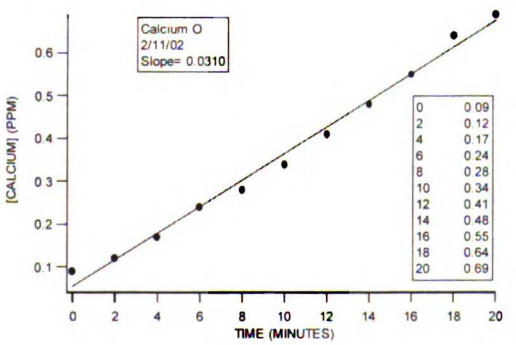

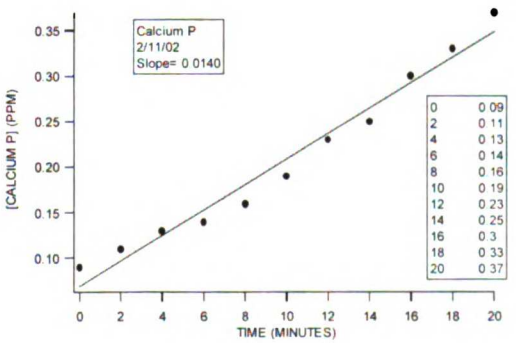

Calcium Dissolution Graphs—Laser and Fluoride

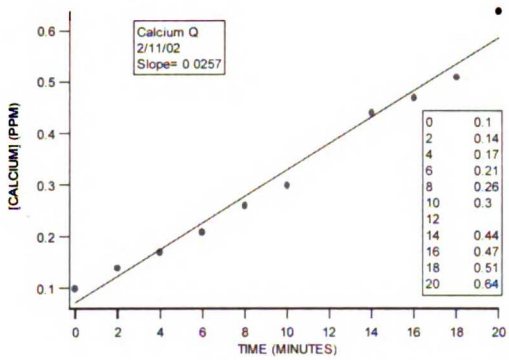

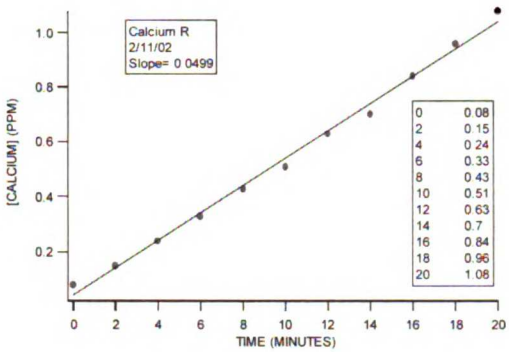

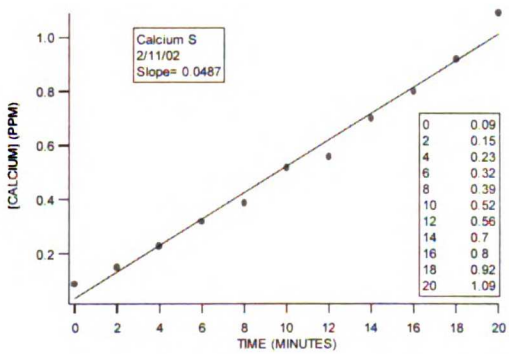

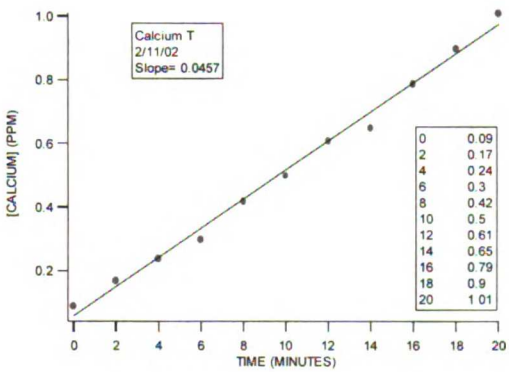

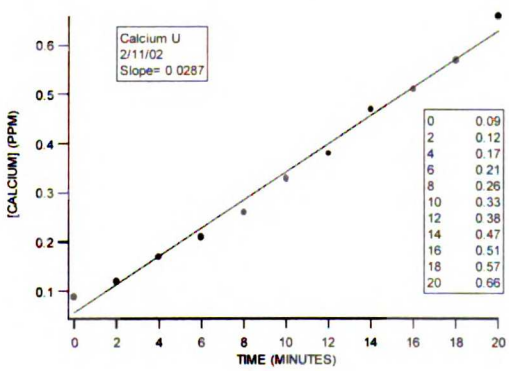

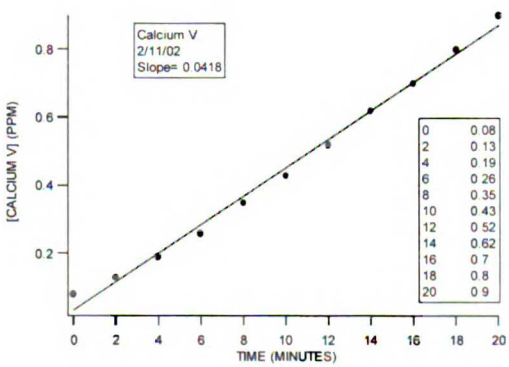

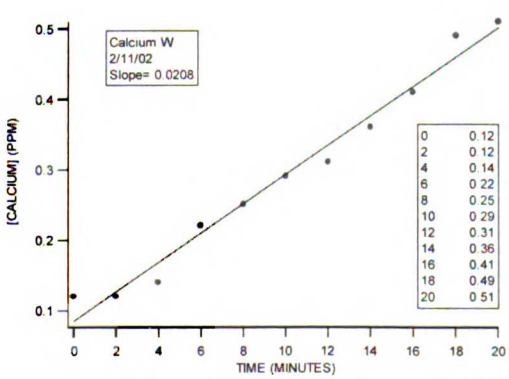

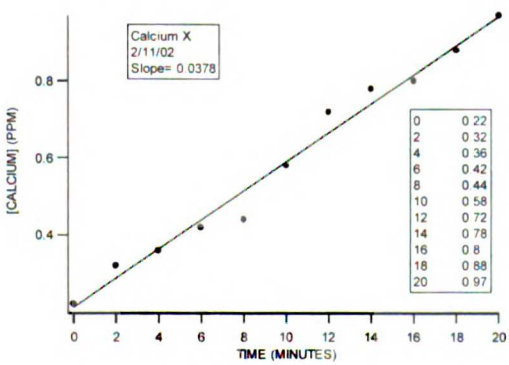

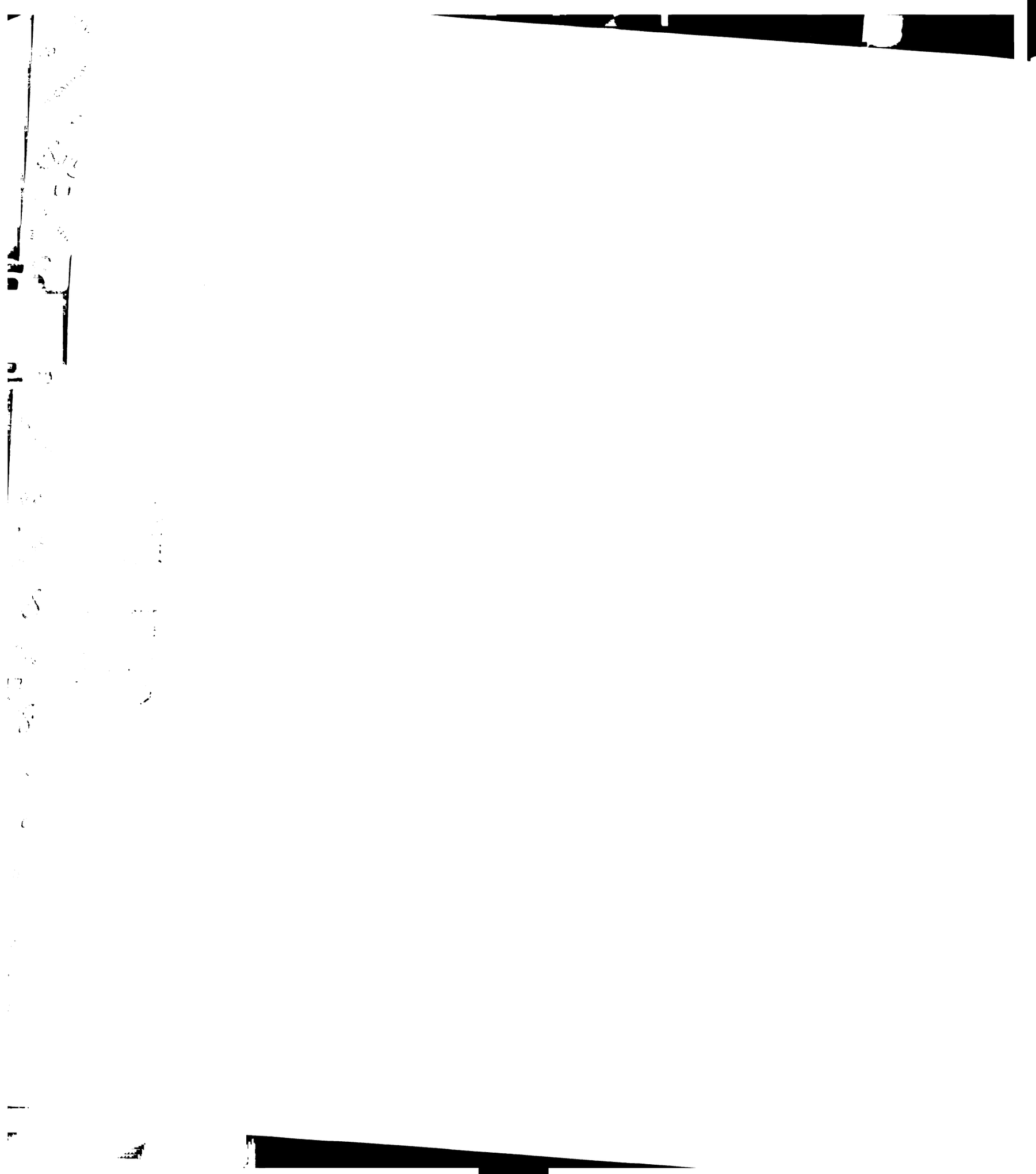

Bond Strengths Tested Under Shear Load Forces

Sample #	Initial Fluence (Mv)	Ending Fluence (Mv)	Average Fluence (Mv)	Shear Force (Kg)	Shear Force Mpa	
A	Low Fluence Group/Suprathreshold approx. 2 J/cm2			*Discarded		
100	13.6	13.6	13.6	14.6	17.7977	
101	12	10	11	9.6	11.7026	
102	13.6	11.9	12.75	15	18.2853	
103	13.6	12.2	12.9	12	14.6282	
104	16.8	12.2	14.5	*	*	
105	17	12	14.5	13.6	16.5787	
106	16.8	12.2	14.5 SD=1.29	15.5	18.8948	SD= 2.6656
107	17.5	11.9	14.7 SE= 0.46	15.5	18.8948	SE= 1.0075
			Mean = 13.56 mV (1.81 J/cm2)		Mean= 16.6832 MPa	
B	Moderate Fluence Group approx. 4 J/cm2					
11	40	27.3	33.65	15.4	18.7729	
12	40	22.8	31.4	14.2	17.3101	
13	40	31	35.5	14	17.0663	
14	40	22	31	13.4	16.3349	
15	34.3	20.1	27.2	13	15.8472	
16	32.3	27.3	29.8	15.8	19.2605	
21	35.2	24.8	30 SD= 2.53	15	18.2853	SD= 1.5082
24	35.2	25.2	30.2 SE= 0.90	12.2	14.872	SE= 0.5332
			Ave = 31.09 mV (4.15 J/cm2)		Mean = 17.2187 MPa	
C	Moderate-High Fluence Group approx. 6.5 J/cm2					
1	49.2	49.2	49.2	14.2	17.3101	
2	49.4	49.4	49.4	17	20.7233	
3	54	48.8	51.4	16.3	19.87	
6	49.4	47	48.2	17	20.7233	
7	49.8	48	48.9	18.6	22.6737	
8	53.8	46.8	50.3	17	20.7233	
9	55	48.2	51.6 SD= 1.34	17	20.7233	SD= 1.6496
10	55	48.2	51.6 SE= 0.47	18.4	22.4299	SE= 0.5832
			Ave = 50.08 mV (6.68 J/cm2)		Mean = 20.6471 MPa	
D	High Fluence Group approx. 8 J/cm2					
30	70.2	52.2	61.2	20	24.3804	
31	71	49	60	16.4	19.9919	
32	78.8	54	66.4	17	20.7233	
33	77.6	54	65.8	18.2	22.1861	
34	78	49	63.5	14.6	17.7977	
36	58	58	58	16.6	20.2357	
37	72.2	52	62.1 SD= 2.97	16.2	19.7481	SD= 2.1043
39	67.4	52	59.7 SE= 1.05	15	18.2853	SE= 0.7440
			Ave = 62.09 mV (8.28 J/cm2)		Mean = 20.4186 MPa	

Phosphate Analysis

													Slope
No Laser, No Fluoride (Control)													
200	0.006	0.008	0.038	0.068	0.104	0.148	0.182	0.232	0.264	0.305	0.35	0.394	0.0437
201	0.005	0.007	0.021	0.036	0.055	0.075	0.094	0.117	0.136	0.158	0.183	0.204	0.0224
202	0.006	0.007	0.009	0.019	0.03	0.04	0.071	0.077	0.088	0.107	0.123	0.143	0.0159
203	0.006	0.008	0.028	0.037	0.051	0.065	0.078	0.098	0.106	0.124	0.135	0.153	0.0158
204	0.005	0.006	0.022	0.036	0.051	0.067	0.091	0.111	0.134	0.155	0.182	0.206	0.0224
205	0.005	0.007	0.019	0.033	0.058	0.078	0.087	0.106	0.125	0.15	0.179	0.202	0.0216
206	0.004	0.004	0.025	0.043	0.064	0.085	0.098	0.12	0.141	0.161	0.18	0.202	0.0219
207	0.004	0.004	0.014	0.021	0.033	0.047	0.06	0.072	0.085	0.102	0.117	0.13	0.0144
	0.0051	0.006	0.022	0.037	0.056	0.076	0.095	0.117	0.135	0.158	0.181	0.204	0.02226
													SD= 0.00929 SE= 0.00328
Laser Only													
A	0.004	0.009	0.029	0.038	0.053	0.092	0.095	0.119	0.147	0.173	0.2	0.23	0.0245
B	0.004	0.011	0.025	0.042	0.064	0.086	0.104	0.129	0.154	0.177	0.205	0.234	0.0247
C	0.008	0.012	0.023	0.037	0.053	0.068	0.087	0.106	0.127	0.145	0.167	0.189	0.02
D	0.003	0.01	0.024	0.042	0.064	0.085	0.109	0.134	0.172	0.194	0.209	0.232	0.0261
E	0.005	0.008	0.021	0.037	0.055	0.074	0.096	0.117	0.142	0.164	0.197	0.23	0.0245
F	0.005	0.011	0.02	0.026	0.034	0.042	0.052	0.063	0.076	0.093	0.105	0.122	0.0122
G	0.004	0.006	0.025	0.034	0.053	0.065	0.083	0.102	0.127	0.145	0.169	0.191	0.0205
H	0.004	0.021	0.029	0.05	0.071	0.095	0.119	0.142	0.164	0.191	0.216	0.242	0.0255
	0.005	0.01	0.025	0.038	0.056	0.076	0.093	0.114	0.139	0.16	0.184	0.209	0.02225
													SD= 0.00464 SE=0.00164
Laser and Fluoride													
I	0.003	0.004	0.008	0.012	0.014	0.022	0.028	0.034	0.041	0.048	0.06	0.063	0.00688
J	0.003	0.014	0.025	0.041	0.056	0.073	0.091	0.113	0.133	0.154	0.18	0.204	0.0214
K	0.003	0.007	0.009	0.009	0.014	0.016	0.019	0.022	0.026	0.029	0.034	0.04	0.00361
L	0.003	0.006	0.009	0.013	0.019	0.024	0.031	0.037	0.043	0.049	0.056	0.062	0.00648
M	0.003	0.009	0.013	0.017	0.021	0.026	0.03	0.036	0.04	0.048	0.054	0.061	0.00575
N	0.003	0.007	0.01	0.014	0.02	0.025	0.031	0.037	0.045	0.053	0.062	0.07	0.00714
O	0.003	0.013	0.017	0.027	0.032	0.044	0.056	0.072	0.085	0.099	0.116	0.131	0.0136
P	0.003	0.005	0.007	0.008	0.012	0.017	0.023	0.029	0.037	0.043	0.052	0.06	0.00633
	0.003	0.008	0.012	0.018	0.024	0.031	0.039	0.048	0.056	0.065	0.077	0.086	0.0089
													SD= 0.00580 SE= 0.00205
Fluoride only													
Q	0.004	0.013	0.011	0.018	0.026	0.036	0.047	0.058	0.075	0.083	0.098	0.111	0.0117
R	0.004	0.006	0.033	0.035	0.053	0.071	0.092	0.112	0.133	0.154	0.177	0.205	0.0216
S	0.005	0.008	0.021	0.037	0.056	0.075	0.095	0.116	0.137	0.159	0.182	0.205	0.0224
T	0.006	0.009	0.021	0.036	0.058	0.069	0.085	0.104	0.123	0.141	0.164	0.184	0.0196
U	0.007	0.006	0.012	0.019	0.027	0.038	0.048	0.06	0.072	0.084	0.095	0.11	0.0117
V	0.007	0.008	0.02	0.03	0.043	0.06	0.079	0.111	0.113	0.135	0.153	0.172	0.0189
W	0.005	0.011	0.015	0.021	0.029	0.037	0.049	0.062	0.066	0.083	0.089	0.1	0.0189
X	0.003	0.008	0.018	0.031	0.047	0.064	0.082	0.101	0.12	0.147	0.158	0.183	0.02
	0.005	0.009	0.019	0.028	0.042	0.056	0.072	0.091	0.105	0.123	0.14	0.159	0.0181
													SD= 0.00414 SE= 0.00146

Calcium Analysis

	0	2	4	6	8	10	12	14	16	18	20	Slope
No Laser, No Fluoride (Control)												
201	0.21	0.27	0.32	0.4	0.52	0.65	0.74	0.83	0.96	1.05	1.17	0.0496
202	0.22	0.27	0.28	0.38	0.44	0.41	0.49	0.6	0.8	0.89	0.99	0.0381
203	0.21	0.41	0.46	0.5	0.55	0.63	0.65	0.76	0.84	0.9	1	0.0349
204	0.22	0.25	0.35	0.44	0.5	0.6	0.73	0.82	1.01	1.08	1.18	0.0504
205	0.17	0.2	0.31	0.34	0.47	0.53	0.63	0.78	0.9	0.99	1.12	0.0487
206	0.17	0.18	0.19	0.25	0.32	0.42	0.53	0.65	0.75	0.89	1	0.044
207	0.23	0.26		0.32	0.4	0.44	0.54	0.56	0.65	0.71	0.75	0.0275
	0.2043	0.2629	0.3183	0.3757	0.4571	0.5257	0.6157	0.7143	0.8443	0.93	1.03	0.0419
												SD= 0.00869 SE= 0.00328
Laser Only												
A	0.11	0.18	0.25	0.36	0.45	0.52	0.69	0.83	0.94	1.1	1.19	0.056
B	0.13	0.2	0.29		0.49	0.6	0.71	0.84	0.94	1.09	1.25	0.0554
C	0.17	0.25	0.31	0.39	0.45	0.6	0.63	0.73	0.83	0.93	1.05	0.0434
D	0.18	0.35	0.43	0.56	0.65	0.73	0.82	1.1	1.18	1.39	1.5	0.0648
E	0.09	0.14	0.22	0.3	0.38	0.49	0.64	0.7	0.79	0.93	1.05	0.0488
F	0.09	0.13	0.17	0.21	0.25	0.29	0.34	0.4	0.47	0.54	0.56	0.0244
G	0.1	0.17	0.23	0.31	0.38	0.48	0.56	0.63	0.75	0.85	0.96	0.0427
H	0.1	0.19	0.31	0.4	0.52	0.63	0.75	0.87	0.98	1.09	1.19	0.0556
	0.1213	0.2013	0.2763	0.3614	0.4463	0.5425	0.6425	0.7625	0.86	0.99	1.0938	0.0489
												SD= 0.0123 SE=0.00435
Laser and Fluoride												
I	0.12	0.14	0.16	0.23	0.24	0.27	0.28	0.4	0.42	0.43	0.44	0.0178
J	0.16	0.18	0.3	0.34	0.38	0.5	0.6	0.72	0.82	0.91		0.0431
K	0.14	0.15	0.16	0.18	0.21	0.22	0.25	0.26	0.27	0.3	0.3	0.00877
L	0.17	0.21	0.2	0.26	0.28	0.28	0.34	0.38	0.42	0.43	0.43	0.0143
M	0.1	0.12	0.13	0.15	0.18	0.2	0.23	0.26	0.3	0.33	0.35	0.013
N	0.09	0.11	0.13	0.17	0.19	0.22	0.25	0.28	0.33	0.38	0.42	0.0164
O	0.09	0.12	0.17	0.24	0.28	0.34	0.41	0.48	0.55	0.64	0.69	0.031
P	0.09	0.11	0.13	0.14	0.16	0.19	0.23	0.25	0.3	0.33	0.37	0.014
	0.12	0.1425	0.1563	0.2138	0.24	0.2775	0.3238	0.3788	0.4263	0.4688	0.4286	0.0198
												SD= 0.01144 SE= 0.00404
Fluoride Only												
Q	0.1	0.14	0.17	0.21	0.26	0.3		0.44	0.47	0.51	0.64	0.0257
R	0.08	0.15	0.24	0.33	0.43	0.51	0.63	0.7	0.84	0.96	1.08	0.0499
S	0.09	0.15	0.23	0.32	0.39	0.52	0.56	0.7	0.8	0.92	1.09	0.0487
T	0.09	0.17	0.24	0.3	0.42	0.5	0.61	0.65	0.79	0.9	1.01	0.0457
U	0.09	0.12	0.17	0.21	0.26	0.33	0.38	0.47	0.51	0.57	0.66	0.0287
V	0.08	0.13	0.19	0.26	0.35	0.43	0.52	0.62	0.7	0.8	0.9	0.0418
W	0.12	0.12	0.14	0.22	0.25	0.29	0.31	0.36	0.41	0.49	0.51	0.0208
X	0.22	0.32	0.36	0.42	0.44	0.58	0.72	0.78	0.8	0.88	0.97	0.0378
	0.1088	0.1625	0.2175	0.2838	0.35	0.4325	0.5329	0.59	0.665	0.7538	0.8575	0.0374
												SD= 0.01109 SE= 0.00392

	[Phosphate]	[Calcium]	Ratio
No Laser, No Fluoride (Control)			
201	0.0224	0.0496	
202	0.0159	0.0381	
203	0.0158	0.0349	
204	0.0224	0.0504	1 to 2.1823
205	0.0216	0.0487	
206	0.0219	0.044	
207	0.0144	0.0275	
Laser Only			
A	0.0245	0.056	
B	0.0247	0.0554	
C	0.02	0.0434	
D	0.0261	0.0648	1 to 2.1978
E	0.0245	0.0488	
F	0.0122	0.0244	
G	0.0205	0.0427	
H	0.0255	0.0556	
Laser and Fluoride			
I	0.00688	0.0178	
J	0.0214	0.0431	
K	0.00361	0.00877	
L	0.00648	0.0143	1 to 2.2247
M	0.00575	0.013	
N	0.00714	0.0164	
O	0.0136	0.031	
P	0.00633	0.014	
	0.0089	0.0198	
Fluoride Only			
Q	0.0117	0.0257	
R	0.0216	0.0499	
S	0.0224	0.0487	
T	0.0196	0.0457	1 to 2.0663
U	0.0117	0.0287	
V	0.0189	0.0418	
W	0.0189	0.0208	
X	0.02	0.0378	
	0.0181	0.0374